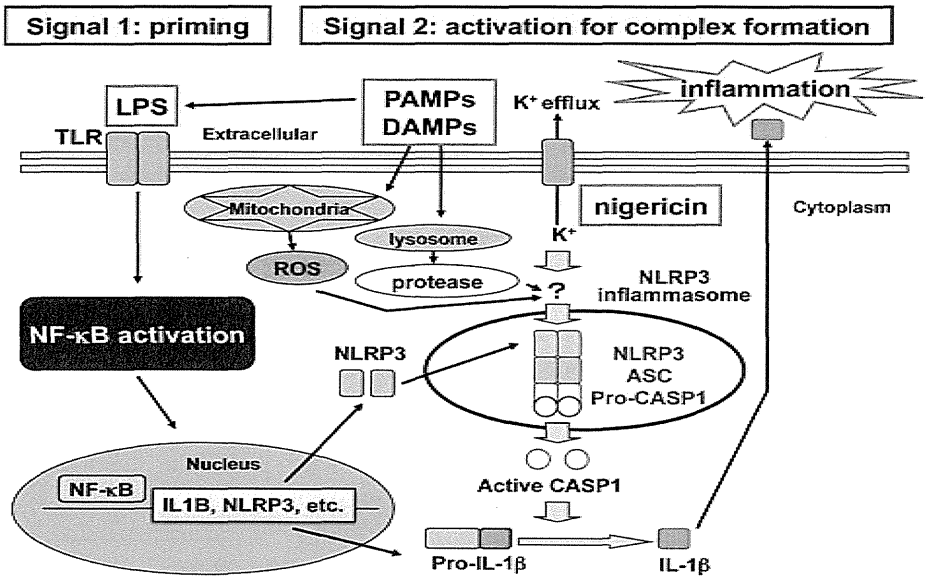

Figure 1: Two-step signals for NLRP3 inflammasome activation. Activation of NLRP3 inflammasome, composed of NLRP3, ASC, and pro-CASP1, is tightly regulated by two-step signals. The first "priming" signal, such as LPS, enhances the expression of inflammasome components and target proteins via activation of transcription factor NF-κB. The second "activation" signal promotes the assembly of inflammasome components. The second signal involves three major mechanisms, including generation of ROS, lysosomal damage, and the potassium efflux. Abbreviations: LPS, lipopolysaccharide; TLR, toll-like receptor; PAMPs, pathogen-associated molecular patterns; DAMPs, danger-associated molecular patterns; ROS, reactive oxygen species.

mitochondrial DNA directly activates NLRP3 inflammasome following induction of apoptosis [6]. By serving as an inducer of two-step signals, a diverse range of danger signals armed with PAMPs, such as *Listeria monocytogenes*, *Candida albicans*, and influenza A virus and those with DAMPs, such as amyloid-β (Aβ), uric acid and cholesterol crystals, asbestos, silica, alum, hyaluronan, and adenosine 5'-triphosphate (ATP), promptly activate the NLRP3 inflammasome [7,8].

Deregulated activation of NLRP3 inflammasome contributes to the pathological processes of various diseases, such as type 2 diabetes, Alzheimer's disease (AD), and multiple sclerosis (MS) [9-11]. Lack of NLRP3 inflammasome components skews microglial cells to an anti-inflammatory M2 phenotype with an enhanced capacity of amyloid-β (Aβ) clearance in a mouse model of AD [10]. *Nlrp3*-knockout mice showed reduced severity of experimental autoimmune encephalomyelitis (EAE), a mouse model of MS, characterized by substantial attenuation of inflammation, demyelination and astrogliosis [12]. In active inflammatory demyelinating lesions of MS, reactive astrocytes and perivascular macrophages expressed all three components of NLRP3 inflammasome, such as NLRP3, ASC, and CASP1, along with IL-1β, suggesting that biochemical agents and monoclonal antibodies designed to block specifically NLRP3 inflammasome activation might be highly effective in treatment of active MS [11]. However, at present, the precise mechanism regulating NLRP3 inflammasome activation and deactivation remains largely unknown. In the present study, by genome-wide gene expression profiling, we attempts to clarify the comprehensive molecular network of NLRP3 inflammasome activation-responsive genes in a human monocyte cell line given consecutively two-step signals.

Materials and Methods

NLRP3 inflammasome activation

A human monocyte cell line THP-1 was obtained from RIKEN Cell Bank (Saitama, Japan). The cells were maintained in RPMI 1640 medium (Invitrogen, Carlsbad, CA, USA) supplemented with 10% fetal bovine serum (FBS), 55 μM 2-mercaptoethanol, 2 mM L-glutamine, 100 U/ml penicillin and 100 μg/ml streptomycin (feeding medium). To load the Signal 1, the cells were incubated for 3 hours with or without 0.2 μg/ml lipopolysaccharide (LPS; Sigma, St. Louis, MO, USA). To load the Signal 2, they were washed twice by Phosphate-Buffered Saline (PBS) and incubated further for 0.5 or 2 hours with 10 μM nigericin sodium salt (Wako Pure Chemical, Osaka, Japan) dissolved in ethanol or the equal v/v% concentration of ethanol (vehicle). Then, protein extract of the cells was processed for western blot analysis with a rabbit antibody against the C-terminal peptide of the human CASP1 p10 protein (sc-515, Santa Cruz Biotechnology, Santa Cruz, CA, USA) and a rabbit antibody against the peptide mapping at amino acid residues of 117-269 of the human IL-1β protein (sc-7884, Santa Cruz Biotechnology).

Microarray analysis

Total cellular RNA was isolated by using the TRIZOL plus RNA Purification kit (Invitrogen). The quality of total RNA was evaluated on Agilent 2100 Bioanalyzer (Agilent Technologies, Palo Alto, CA, USA). Three hundred ng of total RNA was processed for cDNA synthesis, fragmentation, and terminal labeling with the GeneChip Whole Transcript Sense Target Labeling and Control Reagents (Affymetrix, Santa Clara, CA, USA). Then, the labeled cRNA was processed for hybridization at 45°C for 17 hours with Human Gene 1.0 ST Array (28,869 genes; Affymetrix). The arrays were washed in the

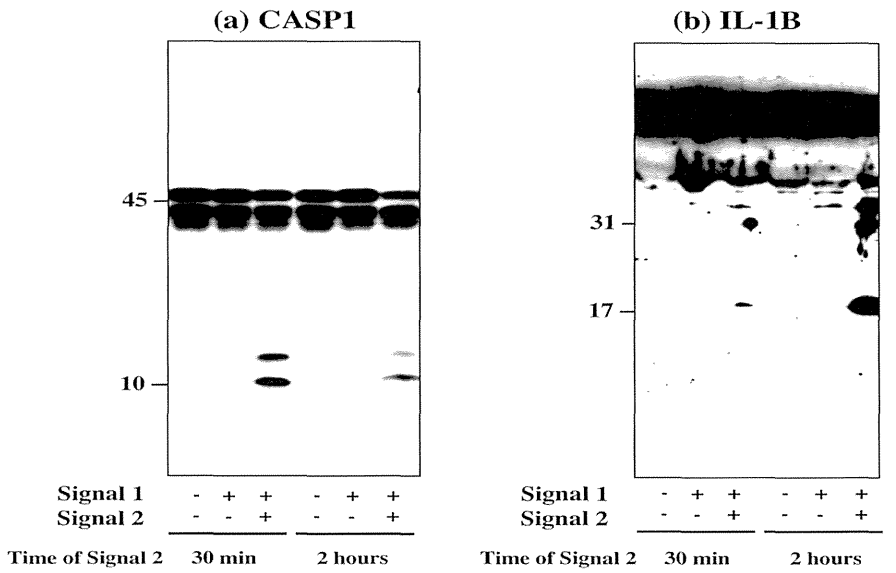

Figure 2: Two-step signals activate NLRP3 inflammasome in THP-1 cells. NLRP3 inflammasome activation was determined by western blot in THP-1 cells following exposure to 0.2 μg/ml LPS for 3 hours (Signal 1), followed by exposure to 10 μM nigericin for 30 min or for 2 hours (Signal 2). The panels **(a, b)** indicate western blot of **(a) CASP1** in the cellular protein extract, and **(b) IL-1β** in the culture supernatant.

Gene Chip Fluidic Station 450 (Affymetrix), and scanned by the Gene Chip Scanner 3000 7G (Affymetrix). The raw data were expressed as CEL files and normalized by the Robust Multi Array average (RMA) method with the Expression Console software (Affymetrix).

Quantitative reverse transcription (RT)-polymerase chain reaction (qPCR) analysis

DNase-treated total RNA isolated from THP-1 cells was processed for cDNA synthesis using oligo(dT)$_{12-18}$ primers and Super Script II reverse transcriptase (Invitrogen). Then, cDNA was amplified by PCR in Light Cycler ST300 (Roche Diagnostics, Tokyo, Japan) using SYBR Green I and a panel of sense and antisense primer sets following: 5'ccagcactgccaaactggactact3' and 5' acagctcagcaaagccagggatct3' for an 162 bp product of nuclear receptor subfamily 4, group A, member 1 (NR4A1); 5'ccaaagccgaccaagacctgcttt3' and 5'ctgtgcaagaccaccccattgcaa3' for an 124 bp product of nuclear receptor subfamily4, group A, member2 (NR4A2); 5'gagggctgcaagggctttttcaag3' and 5' gagggctgagaaggttcctgttgt3' for a 242 bp product of nuclear receptor subfamily 4, group A, member 3 (NR4A3); and 5'ccatgttcgtcatgggtgtgaacca3' and 5'gccagtagaggcagggatgatgttc3' for a 251 bp product of the glyceraldehyde-3-phosphate dehydrogenase (G3PDH) gene that serves as an endogenous control. The expression levels of target genes were standardized against the levels of G3PDH detected in the corresponding cDNA samples. All the assays were performed in triplicate.

Molecular network analysis

To identify biologically relevant molecular networks, we imported corresponding Entrez Gene IDs into Ingenuity Pathways Analysis (IPA) (Ingenuity Systems, Redwood City, CA, USA), KeyMolnet (Institute of Medicinal Molecular Design, Tokyo, Japan), or Search Tool for the Retrieval of Interacting Genes/Proteins (STRING) 9.1. STRING is an open-access database, while IPA and KeyMolnet are commercial resources.

STRING is a database that contains known and predicted, physiological and functional protein-protein interactions composed of 5,214,234 proteins from 1133 organisms [13]. STRING integrates the information from numerous resources, including experimental repositories, computational prediction methods, and public text collections. By uploading the list of UniProt IDs or Gene Symbols, STRING illustrates the union of all possible association networks.

IPA is a knowledgebase that contains approximately 3,000,000 biological and chemical interactions and functional annotations with definite scientific evidence. By uploading the list of Gene IDs and expression values, the network-generation algorithm identifies focused genes integrated in a global molecular network. IPA calculates the score p-value that reflects the statistical significance of association between the genes and the networks by the Fisher's exact test.

KeyMolnet contains knowledge-based contents on 164,000 relationships among human genes and proteins, small molecules, diseases, pathways and drugs [14]. They include the core contents collected from selected review articles with the highest reliability. By importing the list of Gene ID and expression values, KeyMolnet automatically provides corresponding molecules as nodes on the network. The neighboring network-search algorithm selected one or more molecules as starting points to generate the network of all kinds of molecular interactions around starting molecules, including direct activation/inactivation, transcriptional activation/repression, and the complex formation within one path from starting points. The generated network was compared side by side with 501 human canonical pathways of the KeyMolnet library. The algorithm counting the number of overlapping molecular relations between the extracted network and the canonical pathway makes it possible to identify the canonical pathway showing the most significant contribution to the

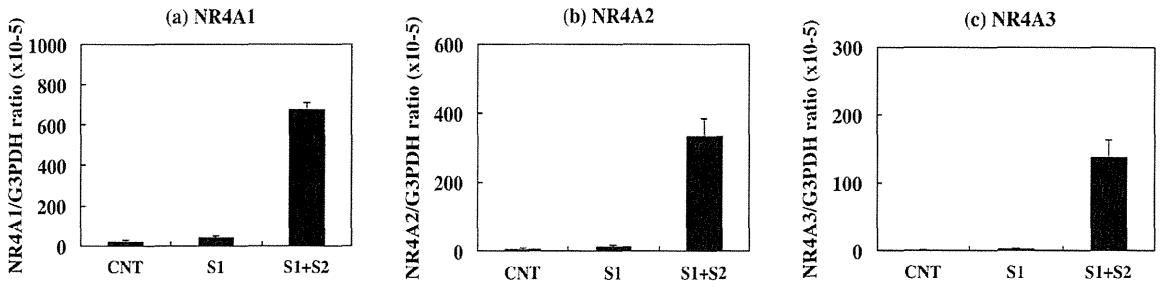

Figure 3: Upregulated expression of NR4A family members in THP-1 cells during NLRP3 inflammasome activation. The levels of expression of NR4A1, NR4A2, and NR4A3 transcripts in THP-1 cells following exposure to 0.2 μg/ml LPS for 3 hours (Signal 1; S1), followed by exposure to 10 μM nigericin for 2 hours (Signal 2; S2) were determined by qPCR. They were standardized against the levels of G3PDH detected in the corresponding cDNA samples. The panels **(a-c)** indicate qPCR of **(a) NR4A1**, **(b) NR4A2**, and **(c) NR4A3**. The bars represent **CNT** (LPS -, nigericin -), **S1** (LPS +, nigericin -), and **S1+S2** (LPS+, nigericin +).

extracted network.

Results

NLRP3 inflammasome activation in THP-1 cells following introduction of two-step signals

First, by western blot analysis, we studied NLRP3 inflammasome activation in THP-1 treated initially with exposure to 0.2 μg/ml LPS for 3 hours (Signal 1), followed by exposure to 10 μM nigericin for 30 min or 2 hours (Signal 2). The consecutive load of Signal 1 and Signal 2 markedly activated NLRP3 inflammasome in THP-1 cells, as indicated by production of cleaved products of CASP1 (Figure 2, panel a) and IL-1β (Figure 2, panel b). In contrast, the introduction of Signal 1 alone was not enough to activate NLRP3 inflammasome in THP-1 cells (Figure 2, panels a and b).

Gene expression profile during NLRP3 inflammasome activation

Next, we studied the genome-wide gene expression profile of THP-1 cells pretreated with 0.2 μg/ml LPS for 3 hours (Signal 1), washed by PBS, and exposed to 10 μM nigericin or vehicle for 2 hours (Signal 2). Then, total RNA was immediately processed for gene expression profiling on a Human Gene 1.0 ST Array. To identify NLRP3 inflammasome activation-responsive genes, we extracted the set of 83 annotated and protein-coding genes that satisfied fold change (FC) in Signal 1 (the presence of LPS versus the absence of LPS) smaller than 2-fold and FC in Signal 2 (the presence of nigericin versus the absence of nigericin) greater than 2-fold (Table 1). This gene enrichment procedure minimized the genes that were activated simply by exposure to LPS alone but not directly related to NLRP3 inflammasome activation.

Most notably, three members of NR4A nuclear receptor family, such as NR4A1 (NUR77), NR4A2 (NURR1), and NR4A3 (NOR1), were identified as those ranked within top 10 genes. Coordinated up regulation of NR4A1, NR4A2, and NR4A3 in NLRP3 inflammasome-activated THP-1 cells was validated by qPCR (Figure 3, panels a-c). Signal 1 alone mildly elevated expression of these mRNA levels, whereas introduction of Signal 2 after Signal 1 markedly elevated the levels of NR4A1, NR4A2, and NR4A3 transcripts with a 16-fold, 25-fold, or 51-fold increase, respectively. We also identified early growth response (EGR) family members, such as EGR1, EGR2, and EGR3, which belong to a family of zinc finger transcription factors involved in the regulation of cell growth, differentiation, and survival, NF-κB inhibitor (IκB) family members, such as NFKBIZ, NFKBID, and NFKBIA, along with a panel of pro inflammatory cytokines and chemokines, including CCL3, CCL3L3, IL8, CXCL2, CCL20, IL23A, and TNFSF9, as a subgroup of NLRP3 inflammasome activation-responsive genes.

Molecular network of NLRP3 inflammasome activation responsive genes

Next, by using three different bioinformatics tools for molecular network analysis based on knowledgebase, we studied biologically relevant molecular networks for the set of 83 NLRP3 inflammasome activation-responsive genes in THP-1 cells. The core analysis of IPA identified the networks defined as "Auditory and Vestibular System Development and Function, Embryonic Development, Organ Development" (p = 1.00E-32), "Cell Cycle, Cellular Development, Cell Death and Survival" (p = 1.00E-30) (Figure 4), and "Connective Tissue Disorders, Immunological Disease, Inflammatory Disease" (p = 1.00E-26) as top three most relevant functional networks. These results suggest that NLRP3 inflammasome activation-responsive genes play a pivotal role in cell development, death, and immune and inflammatory responses. KeyMolnet by the neighboring network-search algorithm operating on the core contents extracted the highly complex molecular network composed of 455 molecules and 529 molecular relations. The network showed the most statistically significant relationship with canonical pathways termed as "transcriptional regulation by AP-1" (p = 3.82E-184), "transcriptional regulation by NR4A" (p = 2.28E-105), and "transcriptional regulation by EGR" (p = 2.78E-99) (Figure 5). These results suggest a central role of transcription factors AP-1, NR4A, and EGR in regulation of expression of NLRP3 inflammasome activation-responsive genes, by acting as a hub of the molecular network.

Finally, STRING extracted a protein-protein interaction network, composed of 35 core molecules derived from the set of 83 NLRP3 inflammasome activation-responsive genes in THP-1 cells. In this network, both the set of NR4A family members NR4A1, NR4A2, and NR4A3 and EGR transcription factors EGR1, EGR2, and EGR3 constituted a close and intense protein interaction subnetwork (Figure 6).

Table 1: The set of 83 up-regulated genes in THP-1 monocytes following activation of NLRP3 inflammasome.

Rank	FC Related to Signal 1	FC Related to Signal 2	Entrez Gene ID	Gene Symbol	Gene Name
1	1.06819645	18.61247501	8013	NR4A3	nuclear receptor subfamily 4, group A, member 3
2	1.942378012	12.91651537	6348	CCL3	chemokine (C-C motif) ligand 3
3	1.63109973	11.69111	414062	CCL3L3	chemokine (C-C motif) ligand 3-like 3
4	1.100615838	11.24166642	9308	CD83	CD83 molecule
5	1.819566773	10.85127008	3576	IL8	interleukin 8
6	1.292541852	7.633454043	1960	EGR3	early growth response 3
7	0.948867136	6.576691539	4929	NR4A2	nuclear receptor subfamily 4, group A, member 2
8	1.116320272	5.51767318	3164	NR4A1	nuclear receptor subfamily 4, group A, member 1
9	1.842348508	5.271896351	64332	NFKBIZ	nuclear factor of kappa light polypeptide gene enhancer in B-cells inhibitor, zeta
10	1.268131184	4.992502002	643616	MOP-1	MOP-1
11	1.222058201	4.99018398	1959	EGR2	early growth response 2
12	1.716614387	4.456895103	5734	PTGER4	prostaglandin E receptor 4 (subtype EP4)
13	1.067764134	4.401932449	10746	MAP3K2	mitogen-activated protein kinase kinase kinase 2
14	1.076240121	4.353030131	2920	CXCL2	chemokine (C-X-C motif) ligand 2
15	1.443866138	4.329651804	6364	CCL20	chemokine (C-C motif) ligand 20
16	1.506881527	4.037790353	5743	PTGS2	prostaglandin-endoperoxide synthase 2 (prostaglandin G/H synthase and cyclooxygenase)
17	1.143021068	3.908082725	153020	RASGEF1B	RasGEF domain family, member 1B
18	1.00701348	3.793627448	1958	EGR1	early growth response 1
19	1.188818931	3.318906546	23645	PPP1R15A	protein phosphatase 1, regulatory (inhibitor) subunit 15A
20	0.978133301	3.154899408	65125	WNK1	WNK lysine deficient protein kinase 1
21	1.116953399	3.113268501	84807	NFKBID	nuclear factor of kappa light polypeptide gene enhancer in B-cells inhibitor, delta
22	1.431860551	3.025219884	51561	IL23A	interleukin 23, alpha subunit p19
23	0.654486344	2.985745104	645188	LOC645188	hypothetical LOC645188
24	1.082721348	2.867304268	1843	DUSP1	dual specificity phosphatase 1
25	1.877501415	2.813972064	8870	IER3	immediate early response 3
26	1.458901009	2.788511085	9021	SOCS3	suppressor of cytokine signaling 3
27	0.930381294	2.730662487	728715	LOC728715	ovostatin homolog 2-like
28	1.251031395	2.703465614	2353	FOS	v-fos FBJ murine osteosarcoma viral oncogene homolog
29	1.994627015	2.654181457	27289	RND1	Rho family GTPase 1
30	0.877732964	2.64583117	23499	MACF1	microtubule-actin crosslinking factor 1
31	1.18363314	2.591793912	7538	ZFP36	zinc finger protein 36, C3H type, homolog (mouse)
32	0.768263434	2.584281103	79101	TAF1D	TATA box binding protein (TBP)-associated factor, RNA polymerase I, D, 41kDa
33	1.895682029	2.568793654	90668	LRRC16B	leucine rich repeat containing 16B
34	0.916615124	2.536018037	259296	TAS2R50	taste receptor, type 2, member 50
35	0.895110685	2.535538194	728741	LOC728741	hypothetical LOC728741
36	0.870604266	2.532650507	84319	CMSS1	cms1 ribosomal small subunit homolog (yeast)
37	0.474895831	2.525788794	4072	EPCAM	epithelial cell adhesion molecule
38	1.667878267	2.514873802	1326	MAP3K8	mitogen-activated protein kinase kinase kinase 8
39	1.107775084	2.496005315	8744	TNFSF9	tumor necrosis factor (ligand) superfamily, member 9
40	1.024389944	2.491488658	4616	GADD45B	growth arrest and DNA-damage-inducible, beta
41	0.97810347	2.470592388	2354	FOSB	FBJ murine osteosarcoma viral oncogene homolog B
42	1.017380957	2.461870724	643036	SLED1	RTFV9368
43	1.017380957	2.377675786	2152	F3	coagulation factor III (thromboplastin, tissue factor)

44	1.038770533	2.373054125	1973	EIF4A1	eukaryotic translation initiation factor 4A, isoform 1
45	1.596962012	2.3683134	4792	NFKBIA	nuclear factor of kappa light polypeptide gene enhancer in B-cells inhibitor, alpha
46	0.872659044	2.354224669	1736	DKC1	dyskeratosis congenita 1, dyskerin
47	1.254570022	2.347010028	50515	CHST11	carbohydrate (chondroitin 4) sulfotransferase 11
48	0.818985035	2.34454831	50840	TAS2R14	taste receptor, type 2, member 14
49	0.649089802	2.278082518	85028	SNHG12	small nucleolar RNA host gene 12 (non-protein coding)
50	0.978928228	2.273044623	2889	RAPGEF1	Rap guanine nucleotide exchange factor (GEF) 1
51	0.689249392	2.247537218	55795	PCID2	PCI domain containing 2
52	0.827575589	2.246739728	54765	TRIM44	tripartite motif-containing 44
53	1.067300921	2.243145194	1263	PLK3	polo-like kinase 3 (Drosophila)
54	0.767788042	2.229552244	337867	UBAC2	UBA domain containing 2
55	1.306111439	2.229215371	3759	KCNJ2	potassium inwardly-rectifying channel, subfamily J, member 2
56	1.925222241	2.191743556	80149	ZC3H12A	zinc finger CCCH-type containing 12A
57	0.882964289	2.185060168	58155	PTBP2	polypyrimidine tract binding protein 2
58	1.545906426	2.181251323	56895	AGPAT4	1-acylglycerol-3-phosphate O-acyltransferase 4 (lysophosphatidic acid acyltransferase, delta)
59	1.05509141	2.155321381	10896	OCLM	oculomedin
60	1.05361515	2.15489714	9659	PDE4DIP	phosphodiesterase 4D interacting protein
61	0.986553364	2.153150265	3047	HBG1	hemoglobin, gamma A
62	0.87493697	2.150450624	100507607	NPIPB9	nuclear pore complex interacting protein family, member B9
63	1.201327908	2.147514699	259292	TAS2R46	taste receptor, type 2, member 46
64	0.885483295	2.144478729	51574	LARP7	La ribonucleoprotein domain family, member 7
65	0.970156229	2.132807866	9839	ZEB2	zinc finger E-box binding homeobox 2
66	0.700126731	2.102345827	100133941	CD24	CD24 molecule
67	1.471640204	2.097753274	6303	SAT1	spermidine/spermine N1-acetyltransferase 1
68	0.796744464	2.080051151	9572	NR1D1	nuclear receptor subfamily 1, group D, member 1
69	1.754590053	2.069409283	10129	FRY	furry homolog (Drosophila)
70	1.117049405	2.06451372	5586	PKN2	protein kinase N2
71	1.084905208	2.058951728	339883	C3orf35	chromosome 3 open reading frame 35
72	1.007649566	2.047104863	1195	CLK1	CDC-like kinase 1
73	1.001286612	2.046307571	1185	CLCN6	chloride channel 6
74	1.005938423	2.043756057	338442	HCAR2	hydroxycarboxylic acid receptor 2
75	0.88066058	2.04297423	6144	RPL21	ribosomal protein L21
76	1.048011825	2.039547357	1844	DUSP2	dual specificity phosphatase 2
77	1.361895488	2.039480914	3092	HIP1	huntingtin interacting protein 1
78	0.951119813	2.038925421	388022	LOC388022	hypothetical gene supported by AK131040
79	0.888482949	2.018363478	144132	DNHD1	dynein heavy chain domain 1
80	0.972189862	2.012125102	23049	SMG1	SMG1 homolog, phosphatidylinositol 3-kinase-related kinase (C. elegans)
81	0.89112764	2.007348359	6181	RPLP2	ribosomal protein, large, P2
82	0.798221473	2.005195646	23329	TBC1D30	TBC1 domain family, member 30
83	1.206469961	2.003702064	3726	JUNB	jun B proto-oncogene

To activate NLRP3 inflammasome, THP-1 cells were initially exposed to 0.2 μg/ml LPS for 3 hours (Signal 1). They were then washed by PBS and exposed to 10 μM nigericin for 2 hours (Signal 2 after Signal 1). At 5 hours after initiation of the treatment, total RNA was isolated and processed for gene expression profilong on a Human Gene 1.0 ST Array. The set of 83 genes that satisfy fold change (FC) related to Signal 1 (LPS + versus LPS -) smaller than 2-fold and FC related to Signal 2 (nigericin + versus nigericin -) greater than 2-fold are shown with FC, Entrez Gene ID, Gene Symbol, and Gene Name.

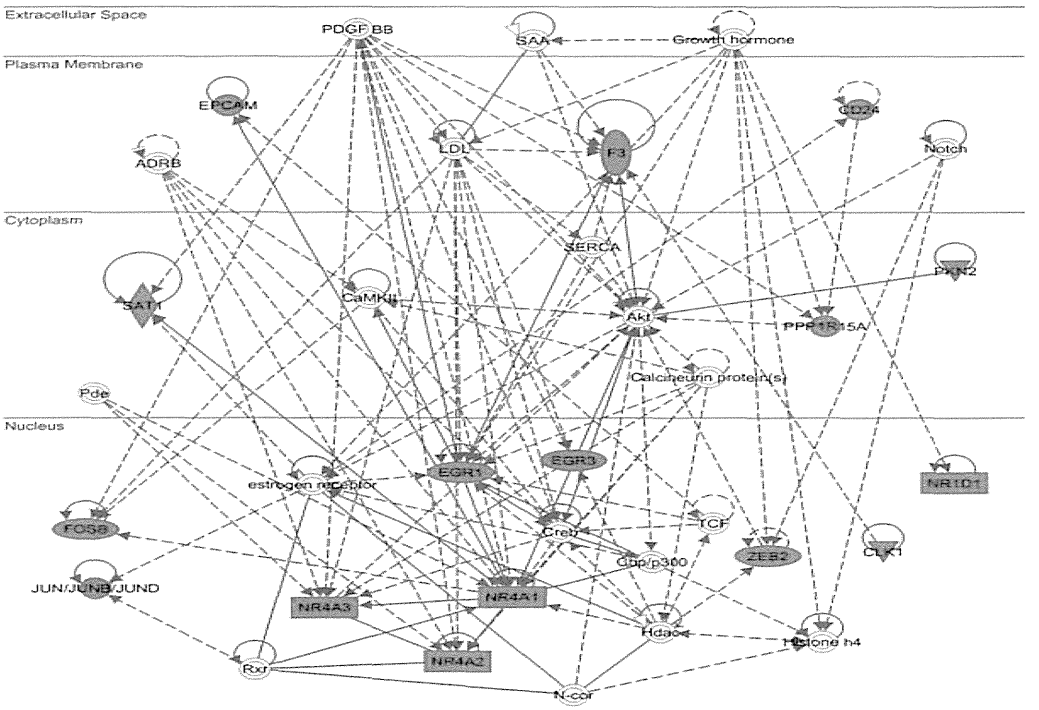

Figure 4: IPA molecular network of NLRP3 inflammasome activation-responsive genes. Entrez Gene IDs corresponding to the set of 83 NLRP3 inflammasome activation-responsive genes in THP-1 cells (Table 1) were imported into the core analysis tool of IPA. The functional network defined as "Cell Cycle, Cellular Development, Cell Death and Survival" is shown. Red nodes indicate NLRP3 inflammasome activation-responsive genes.

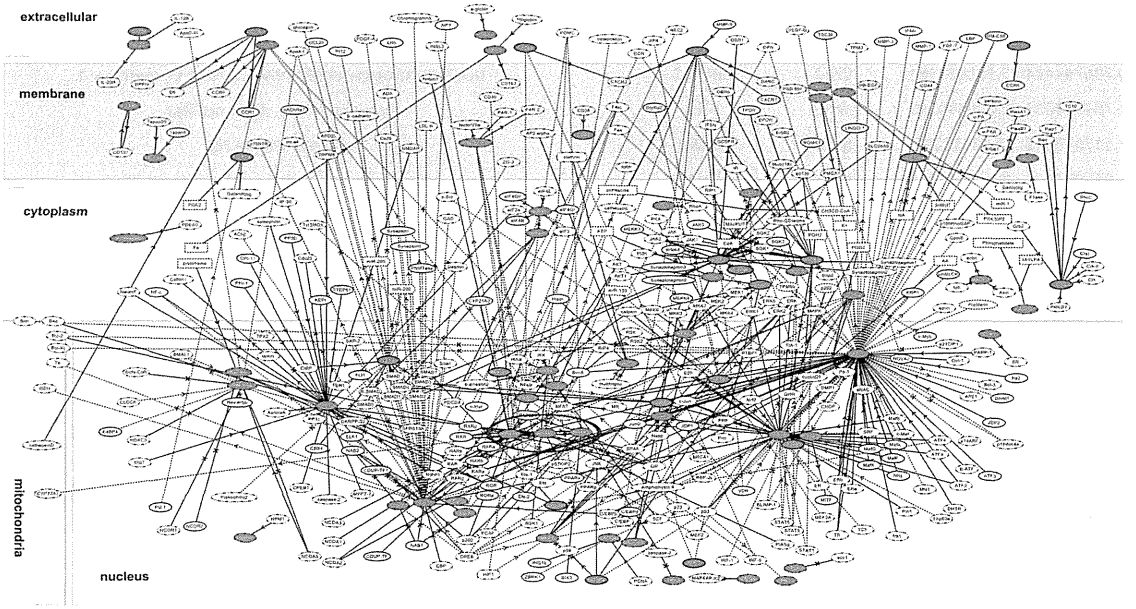

Figure 5: KeyMolnet molecular network of NLRP3 inflammasome activation-responsive genes. Entrez Gene IDs corresponding to the set of 83 NLRP3 inflammasome activation-responsive genes in THP-1 cells (Table 1) were imported into KeyMolnet. The neighboring network-search algorithm operating on the core contents extracted the highly complex molecular network. Red nodes represent NLRP3 inflammasome activation-responsive genes, while white nodes exhibit additional nodes extracted automatically from the core contents of KeyMolnet to establish molecular connections. The molecular relation is indicated by solid line with arrow (direct binding or activation), solid line with arrow and stop (direct inactivation), solid line without arrow (complex formation), dash line with arrow (transcriptional activation), and dash line with arrow and stop (transcriptional repression). The cluster of NR4A1, NR4A2, and NR4A3 is highlighted by blue circle.

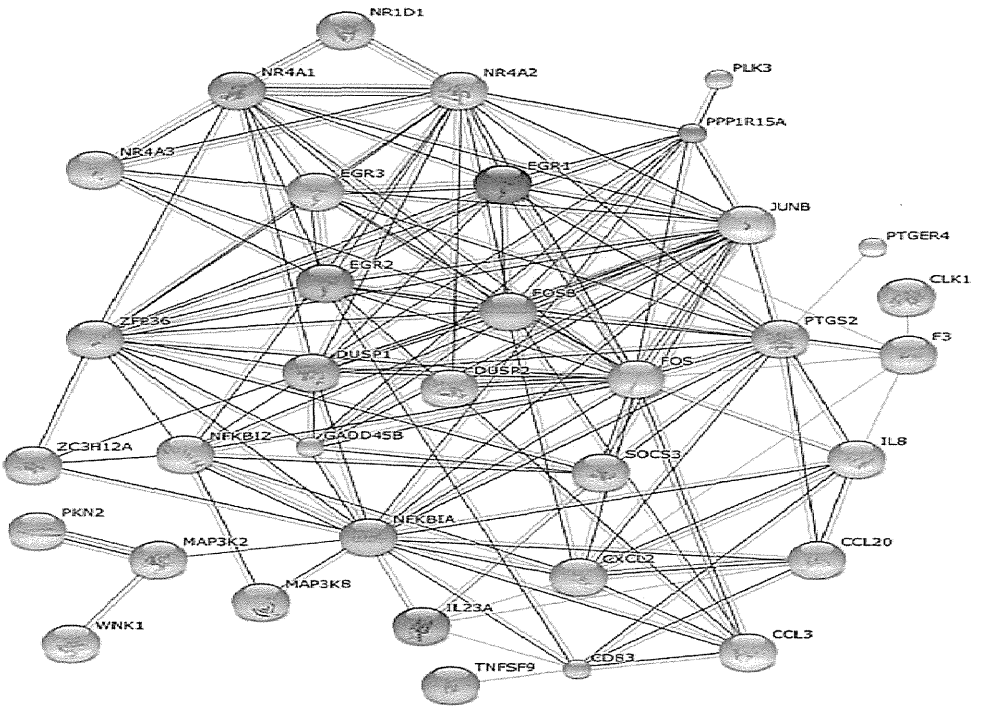

Fig. 6. STRING molecular network of NLRP3 inflammasome activation-responsive genes. Gene Symbols corresponding to the set of 83 NLRP3 inflammasome activation-responsive genes in THP-1 cells (Table 1) were imported into STRING. The set of 35 molecules constructing the protein-protein interaction network are shown on the evidence view of STRING.

Discussion

By genome-wide gene expression profiling, we identified the set of 83 NLRP3 inflammasome activation-responsive genes in THP-1 cells sequentially given two-step signals. Among them, we found three members of NR4A nuclear receptor family, such as NR4A1, NR4A2, and NR4A3, three members of EGR family, such as EGR1, EGR2, and EGR3, three members of IκB family, such as NFKBIZ, NFKBID, and NFKBIA as a noticeable subset of NLRP3 inflammasome activation-responsive genes. By molecular network analysis, we found that they play a central role in cellular development and death, and immune and inflammatory responses, where transcription factors AP-1, NR4A, and EGR serve as a hub in the molecular network. Because THP-1 is a spontaneously immortalized human monocytic cell line derived from an acute monocytic leukemia patient, the possibility could not be excluded that the molecular network we identified does not represent the physiological network of non-malignant human monocytes.

NR4A1, NR4A2, and NR4A3 are three closely related, highly homologous nuclear transcription factors of the steroid/thyroid hormone receptor superfamily, categorized as orphan nuclear receptors because of lack of their cognate ligands [15]. They are encoded by immediate early genes, rapidly induced by exposure of the cells to the serum, growth factors, cytokines, and peptide hormones. NR4A receptors act as a transcription factor for a battery of downstream genes involved in cell proliferation, apoptosis, DNA repair, inflammation, and angiogenesis [16]. Accumulating evidence indicates that NR4A family exerts not only proinflammatory but also anti-inflammatory effects on various cell types. NR4A receptors play a pivotal role in development of regulatory T (Treg) cells in the thymus [17]. Knockdown of either NR4A1 or NR4A3 elevates the levels of production of IL-1β, IL-8, and MCP-1 in THP-1 cells [18]. By binding directly to NF-κB p65, a central regulator of innate and adaptive immune response, NR4A1 recruits the CoREST corepressor complex on gene promoter and inhibits transcription of proinflammatory genes in mouse microglia and astrocytes [19]. Adenosine monophosphate released from apoptotic cells, when metabolized to adenosine, activates macrophages to express NR4A1, NR4A2, and NR4A3 that play a role in suppression of inflammation during engulfment of apoptotic cells [20]. Recently, we found that NR4A2 is one of vitamin D receptor-target genes with protective function against development of MS by analyzing a chromatin immunoprecipitation followed by deep sequencing (ChIP-Seq) dataset derived from immortalized B cells and THP-1 cells [21]. All of these observations suggest that NR4A proteins, whose expression is induced by proinflammatory mediators, serve as a safety valve for shutting down sustained inflammation that is amplified by NLRP3 inflammasome activation. Consistent with this view, IκB family members acting as a negative regulator of NF-κB activation, such as NFKBIZ, NFKBID, and NFKBIA [22-24], are coordinately induced along with enhanced expression of NR4A family, suggesting that these molecules constitute a negative feedback loop for NLRP3 inflammasome activation.

EGR family constitutes a family of zinc finger transcription factors very rapidly and transiently induced in various cell types without *de novo* protein synthesis following exposure to mitogenic signals [25,26]. EGR1 functions as a positive regulator for T and B cell functions, by regulating transcription of the genes encoding key cytokines and costimulatory molecules, while EGR2 and EGR3 act as a negative regulator essential for induction of anergy [27]. EGR1 downregulates the expression of itself by binding to an EGR1-binding site located on its own promoter [28]. Furthermore, EGR1 directly activates transcription of NR4A1 (nur77) in mouse IgM^+ B cells [29]. Deletion of EGR2 and EGR3 in mouse T and B cells causes a lethal autoimmune syndrome characterized by excessive production of proinflammatory cytokines accompanied by overactivation of STAT1 and STAT3 [30]. Importantly, we identified SOCS3, a potent inhibitor of STAT3 activation [31], as one of NLRP3 inflammasome activation-responsive genes (Rank 26 in Table 1). These observations suggest the working hypothesis that the EGR family members are actively involved in resolution of sustained inflammation amplified by NLRP3 inflammasome activation.

Conclusion

By genome-wide gene expression profiling, we identified the set of 83 NLRP3 inflammasome activation-responsive genes in THP-1 cells. Among them, we found NR4A nuclear receptor family, EGR family, and IκB family as a group of the genes that possibly constitute a negative feedback loop for shutting down sustained inflammation following NLRP3 inflammasome activation. By molecular network analysis, we found that NLRP3 inflammasome activation-responsive genes play a pivotal role in cellular development and death, and immune and inflammatory responses, where transcription factors AP-1, NR4A, and EGR act as a hub in the molecular network.

Acknowledgement

This work was supported by the JSPS KAKENHI (C25430054), and the Intractable Disease Research Center (IDRC) project, the Ministry of Education, Culture, Sports, Science and Technology (MEXT), Japan, and the grant from the National Center for Geriatrics and Gerontology (NCGC 26-20). The authors would thank Ms. Aki Takaoka for her invaluable help in microarray analysis. The microarray data are available from the Gene Expression Omnibus (GEO) under the accession number GSE58959.

References

1. Schroder K, Tschopp J. The inflammasomes. Cell. 2010; 140: 821-832.
2. Menu P, Vince JE. The NLRP3 inflammasome in health and disease: the good, the bad and the ugly. Clin Exp Immunol. 2011; 166: 1-15.
3. Wang H, Mao L, Meng G. The NLRP3 inflammasome activation in human or mouse cells, sensitivity causes puzzle. Protein Cell. 2013; 4: 565-568.
4. Walsh JG, Muruve DA, Power C. Inflammasomes in the CNS. Nat Rev Neurosci. 2014; 15: 84-97.
5. Zhou R, Yazdi AS, Menu P, Tschopp J. A role for mitochondria in NLRP3 inflammasome activation. Nature. 2011; 469: 221-225.
6. Shimada K, Crother TR, Karlin J, Dagvadorj J, Chiba N, Chen S, et al. Oxidized mitochondrial DNA activates the NLRP3 inflammasome during apoptosis. Immunity. 2012; 36: 401-414.
7. Di Virgilio F. Liaisons dangereuses: P2X(7) and the inflammasome. Trends Pharmacol Sci. 2007; 28: 465-472.
8. Halle A, Hornung V, Petzold GC, Stewart CR, Monks BG, Reinheckel T, et al. The NALP3 inflammasome is involved in the innate immune response to amyloid-beta. Nat Immunol. 2008; 9: 857-865.
9. Jourdan T, Godlewski G, Cinar R, Bertola A, Szanda G, Liu J, et al. Activation of the Nlrp3 inflammasome in infiltrating macrophages by endocannabinoids mediates beta cell loss in type 2 diabetes. Nat Med. 2013; 19: 1132-1140.
10. Heneka MT, Kummer MP, Stutz A, Delekate A, Schwartz S, Vieira-Saecker A, Griep A. NLRP3 is activated in Alzheimer's disease and contributes to pathology in APP/PS1 mice. Nature. 2013; 493: 674-678.
11. Kawana N, Yamamoto Y, Ishida T, Saito Y, Konno H, Arima K, et al. Reactive astrocytes and perivascular macrophages express NLRP3 inflammasome in active demyelinating lesions of multiple sclerosis and necrotic lesions of neuromyelitis optica and cerebral infarction. Clin Exp Neuroimmunol. 2013; 4: 296-304.
12. Gris D, Ye Z, Iocca HA, Wen H, Craven RR, Gris P, Huang M. NLRP3 plays a critical role in the development of experimental autoimmune encephalomyelitis by mediating Th1 and Th17 responses. J Immunol. 2010; 185: 974-981.
13. Franceschini A, Szklarczyk D, Frankild S, Kuhn M, Simonovic M, Roth A, Lin J. STRING v9.1: protein-protein interaction networks, with increased coverage and integration. Nucleic Acids Res. 2013; 41: D808-815.
14. Satoh J. Bioinformatics approach to identifying molecular biomarkers and networks in multiple sclerosis. Clin Exp Neuroimmunol. 2010; 1: 127–140.
15. Zhao Y, Bruemmer D. NR4A orphan nuclear receptors: transcriptional regulators of gene expression in metabolism and vascular biology. Arterioscler Thromb Vasc Biol. 2010; 30: 1535-1541.
16. Mohan HM, Aherne CM, Rogers AC, Baird AW, Winter DC, Murphy EP. Molecular pathways: the role of NR4A orphan nuclear receptors in cancer. Clin Cancer Res. 2012; 18: 3223-3228.
17. Sekiya T, Kashiwagi I, Yoshida R, Fukaya T, Morita R, Kimura A, Ichinose H. Nr4a receptors are essential for thymic regulatory T cell development and immune homeostasis. Nat Immunol. 2013; 14: 230-237.
18. Bonta PI, van Tiel CM, Vos M, Pols TW, van Thienen JV, Ferreira V, et al. Nuclear receptors Nur77, Nurr, and NOR-1 expressed in atherosclerotic lesion macrophages reduce lipid loading and inflammatory responses. Arterioscler Thromb Vasc Biol. 2006; 26: 2288-2294.
19. Saijo K, Winner B, Carson CT, Collier JG, Boyer L, Rosenfeld MG, et al. A Nurr1/CoREST pathway in microglia and astrocytes protects dopaminergic neurons from inflammation-induced death. Cell. 2009; 137: 47-59.
20. Yamaguchi H, Maruyama T, Urade Y, Nagata S. Immunosuppression via adenosine receptor activation by adenosine monophosphate released from apoptotic cells. Elife. 2014; 3: e02172.
21. Satoh J, Tabunoki H. Molecular network of chromatin immunoprecipitation followed by deep sequencing-based vitamin D receptor target genes. Mult Scler. 2013; 19: 1035-1045.
22. Muta T, Yamazaki S, Eto A, Motoyama M, Takeshige K. IkappaB-zeta, a new anti-inflammatory nuclear protein induced by lipopolysaccharide, is a negative regulator for nuclear factor-kappaB. J Endotoxin Res. 2003; 9: 187-191.
23. Tergaonkar V, Correa RG, Ikawa M, Verma IM. Distinct roles of IkappaB proteins in regulating constitutive NF-kappaB activity. Nat Cell Biol. 2005; 7: 921-923.
24. Kuwata H, Matsumoto M, Atarashi K, Morishita H, Hirotani T, Koga R, et al. IkappaBNS inhibits induction of a subset of Toll-like receptor-dependent genes and limits inflammation. Immunity. 2006; 24: 41-51.
25. Christy B, Nathans D. DNA binding site of the growth factor-inducible protein Zif268. Proc Natl Acad Sci U S A. 1989; 86: 8737-8741.
26. Beckmann AM, Wilce PA. Egr transcription factors in the nervous system. Neurochem Int. 1997; 31: 477-510.
27. Gómez-Martín D, Díaz-Zamudio M, Galindo-Campos M, Alcocer-Varela J. Early growth response transcription factors and the modulation of immune

response: implications towards autoimmunity. Autoimmun Rev. 2010; 9: 454-458.

28. Cao X, Mahendran R, Guy GR, Tan YH. Detection and characterization of cellular EGR-1 binding to its recognition site. J Biol Chem. 1993; 268: 16949-16957.

29. Dinkel A, Warnatz K, Ledermann B, Rolink A, Zipfel PF, Bürki K, et al. The transcription factor early growth response 1 (Egr-1) advances differentiation of pre-B and immature B cells. J Exp Med. 1998; 188: 2215-2224.

30. Li S, Miao T, Sebastian M, Bhullar P, Ghaffari E, Liu M, et al. The transcription factors Egr2 and Egr3 are essential for the control of inflammation and antigen-induced proliferation of B and T cells. Immunity. 2012; 37: 685-696.

31. Carow B, Rottenberg ME. SOCS3, a Major Regulator of Infection and Inflammation. Front Immunol. 2014; 5: 58.

Austin J Clin Immunol - Volume 1 Issue 4 - 2014
Submit your Manuscript | www.austinpublishinggroup.com

Citation: Kawana N, Yamamoto Y, Kino Y and Jun-ichi Satoh. Molecular Network of NLRP3 Inflammasome Activation-Responsive Genes in a Human Monocyte Cell Line. Austin J Clin Immunol. 2014;1(4): 10.

Satoh et al. Alzheimer's Research & Therapy 2014, 6:17
http://alzres.com/content/6/2/17

alzheimer's research&therapy

RESEARCH Open Access

TMEM106B expression is reduced in Alzheimer's disease brains

Jun-ichi Satoh[1*], Yoshihiro Kino[1], Natsuki Kawana[1], Yoji Yamamoto[1], Tsuyoshi Ishida[2], Yuko Saito[3] and Kunimasa Arima[4]

Abstract

Introduction: TMEM106B is a transmembrane glycoprotein of unknown function located within endosome/lysosome compartments expressed ubiquitously in various cell types. Previously, the genome-wide association study (GWAS) identified a significant association of *TMEM106B* single nucleotide polymorphisms (SNPs) with development of frontotemporal lobar degeneration with ubiquitinated TAR DNA-binding protein-43 (TDP-43)-positive inclusions (FTLD-TDP), particularly in the patients exhibiting the progranulin (PGRN) gene (*GRN*) mutations. Recent studies indicate that TMEM106B plays a pathological role in various neurodegenerative diseases, including Alzheimer's disease (AD). However, at present, the precise levels of TMEM106B expression in AD brains remain unknown.

Methods: By quantitative reverse transcription (RT)-PCR (qPCR), western blot and immunohistochemistry, we studied TMEM106B and PGRN expression levels in a series of AD and control brains, including amyotrophic lateral sclerosis, Parkinson's disease, multiple system atrophy and non-neurological cases.

Results: In AD brains, TMEM106B mRNA and protein levels were significantly reduced, whereas PGRN mRNA levels were elevated, compared with the levels in non-AD brains. In all brains, TMEM106B was expressed in the majority of cortical neurons, hippocampal neurons, and some populations of oligodendrocytes, reactive astrocytes and microglia with the location in the cytoplasm. In AD brains, surviving neurons expressed intense TMEM106B immunoreactivity, while senile plaques, neurofibrillary tangles and the perivascular neuropil, almost devoid of TMEM106B, intensely expressed PGRN.

Conclusions: We found an inverse relationship between TMEM106B (downregulation) and PGRN (upregulation) expression levels in AD brains, suggesting a key role of TMEM106B in the pathological processes of AD.

Introduction

Frontotemporal lobar degeneration (FTLD) provides the second most common cause of presenile dementia worldwide. The first international genome-wide association study of FTLD with ubiquitinated TAR DNA-binding protein-43-positive inclusions (FTLD-TDP) identified a significant association with three distinct single nucleotide polymorphisms (SNPs) numbered rs1020004, rs6966915, and rs1990622 (top SNP) in the transmembrane protein 106B (*TMEM106B*) gene on chromosome 7p21.3 [1]. The study also found that TMEM106B mRNA levels are elevated by greater than 2.5-fold in the frontal cortex of FTLD-TDP patients, compared with the levels of normal subjects. The minor C allele on rs1990622 in the *TMEM106B* gene confers significant protection against development of FTLD, most notably in the patients with the progranulin (PGRN) gene (*GRN*) mutations [1]. This association is replicated in independent cohorts [2,3]. A number of previous studies showed that all *GRN* mutations cause FTLD-TDP by the mechanism of haploinsufficiency due to nonsense-mediated decay of mutated mRNAs [4,5]. A different study validated a substantial increase in TMEM106B mRNA and protein levels in FLTD-TDP brains with *GRN* mutations [6].

TMEM106B is a type II transmembrane glycoprotein of unknown function located within the late endosome/lysosome compartments expressed ubiquitously in various cell types, where the levels of TMEM106B expression are regulated by lysosomal activities [7,8]. In rat neurons in culture, TMEM106B plays a pivotal role in dendritic trafficking

* Correspondence: satoj@my-pharm.ac.jp
[1]Department of Bioinformatics and Molecular Neuropathology, Meiji Pharmaceutical University, 2-522-1 Noshio, Kiyose, Tokyo 204-8588, Japan
Full list of author information is available at the end of the article

of lysosomes [9]. PGRN is a secreted glycoprotein with pleitropic functions involved in embryogenesis, oncogenesis, and inflammation, widely expressed in epithelial cells of the skin, gastrointestinal tract and the reproductive system, leukocytes, and neurons in the central nervous system [10,11]. Sortilin, serving as a cell-surface receptor for PGRN, regulates trafficking and targeting of PGRN to lysosomes [12]. The risk T allele on rs1990622 in the *TMEM106B* gene is linked to low plasma PGRN levels, suggesting that *TMEM106B* SNPs modulate secreted levels of PGRN [13,14]. A nonsynonymous SNP numbered rs3173615 (p.T185S) located in exon 6 of the *TMEM106B* gene shows complete linkage disequilibrium with rs1990622 [3,13,15]. The expression levels of the protective isoform S185 are always lower than those of the risk isoform T185, attributable to accelerated degradation of the S185 protein, suggesting that increased expression of the T185 protein might perturb the endolysosomal pathway [3]. Actually, overexpression of TMEM106B induces enlargement of lysosomes and inhibits lysosomal degradation of PGRN [8]. Importantly, the frequency of carriers homozygous for S185 on rs3173615 is reduced in the patients with C9orf72 repeat expansions, the most common genetic cause for FTLD [15], whereas the risk T allele on rs1990622 is positively associated with later age at onset and death in C9orf72 repeat expansion carriers [16].

A recent study showed that TMEM106B genotypes influence the development of cognitive impairment in amyotrophic lateral sclerosis (ALS) patients [17]. The risk T allele on rs1990622 in the *TMEM106B* gene is significantly associated with poor cognitive performance in ALS patients. Furthermore, the frequency of the protective C allele on rs1990622 is reduced in Alzheimer's disease (AD) cases presenting with TDP-43 pathology [18]. The interplay between TMEM106B and APOE genotypes increases AD risk in a Han Chinese population [19]. All of these observations suggest that TMEM106B plays a key role in the pathology not only of FTLD-TDP but also of other neurodegenerative diseases, such as AD. The precise levels of TMEM106B expression in AD brains, however, remain unknown at present. In the present study, we characterized TMEM106B and PGRN expression levels in AD and non-AD brains by quantitative reverse transcriptase-polymerase chain reaction (qPCR), western blot and immunohistochemistry. We found that the levels of TMEM106B expression are substantially reduced, while those of PRGN are elevated in AD brains.

Materials and methods

Human brain tissues

The serial sections of the frontal cortex and the hippocampus were prepared from autopsied brains of six sporadic AD patients, composed of three men and three women with a mean age of 73 ± 9 years, and 13 non-AD patients, composed of six men and seven women with a mean age of 74 ± 8 years, as described previously [20]. The non-AD group includes four normal subjects that died of non-neurological causes (NC), three patients with sporadic Parkinson's disease (PD), four patients with sporadic ALS, and two patients with sporadic multiple system atrophy (MSA). The demographic profile of the cases examined is presented in Table 1. All AD cases met with the Consortium to Establish a Registry for Alzheimer's Disease criteria for diagnosis of definite AD [21]. They were categorized into stage C of amyloid deposition and into stage VI of neurofibrillary degeneration, following the Braak staging system [22]. Autopsies on all subjects were performed at the National Center Hospital, National Center of Neurology and Psychiatry, Japan or the Kohnodai Hospital, National Center for Global Health and Medicine, Japan. In all cases, written informed consent was obtained. The Ethics Committee of the National Center of Neurology and Psychiatry for the Human Brain Research, the Ethics Committee of the National Center for Global Health and Medicine on the Research Use of Human Samples, and the Human Research Ethics Committee of the Meiji Pharmaceutical University approved the present study.

Immunohistochemistry

The brain tissues were fixed with 4% paraformaldehyde and embedded in paraffin. After deparaffination, tissue sections were heat-treated in 10 mM citrate sodium buffer, pH 6.0, by autoclaving at 110°C for 15 minutes in a temperature-controlled pressure chamber (Biocare Medical, Concord, CA, USA). The sections were processed for immunohistochemistry, according to the methods described previously [23]. In brief, the tissue sections were incubated at room temperature for 15 minutes with 3% hydrogen peroxide-containing methanol to block the endogenous peroxidase activity, and were also incubated with phosphate-buffered saline containing 10% normal goat or rabbit serum at room temperature for 15 minutes to block nonspecific staining. The sections were then incubated at 4°C overnight with a rabbit polyclonal anti-TMEM106B antibody raised against a peptide spanning amino acid residues 1 to 50 of the human TMEM106B protein at a concentration of 0.1 μg/ml (A303-439A; Bethyl Laboratories, Montgomery, TX, USA), a rabbit monoclonal anti-PGRN antibody raised against a synthetic peptide corresponding to the residues in the human PGRN protein at a dilution of 1:1,000 (EPR3781; Abcam, Cambridge, UK), or a mouse monoclonal anti-pS409/410 TDP-43 antibody raised against a phosphopeptide composed of CMDSKpSpSGWGM at a dilution of 1:500 (TIP-PTD-M01; Cosmo Bio, Tokyo, Japan). The specificity of A303-439A and EPR3781 antibodies was validated individually by western blot analysis of the corresponding recombinant proteins expressed in human cell lines in culture. After washing with

Table 1 Demographic profile of the cases examined in the present study

Case number	IHC	qPCR/WB	Cause of death	Brain weight (grams)	Postmortem interval (hours)	Braak staging (amyloid deposition/ neurofibrillary degeneration)	pTDP-43 immunoreactivity		p.T185S genotype
							Frontal cortex	Hippocampus	
NC1	+	+	Acute myocardial infarction	1,130	1.4	A/II	–	–	T/T
NC2	+	+	Acute myocardial infarction	1,350	1.6	0/II	–	–	T/S
NC3	+	+	Lung cancer	1,060	3.9	A/II	–	–	T/S
NC4	+	+	Dissecting aortic aneurysm	1,400	4.8	A/I	–	–	T/T
AD1	+	+	Pneumonia	1,000	1.1	C/VI	+	+	T/S
AD2		+	Pneumonia	1,230	14	C/VI			T/S
AD3	+	+	Pneumonia	1,220	10.5	C/VI	–	+	T/S
AD4	+	+	Pneumonia	1,240	8.1	C/VI	–	–	T/S
AD5	+	+	Lung cancer	1,090	4.5	C/VI	–	–	T/T
AD6	+	+	Pulmonary infarction	840	3	C/VI	–	+	T/S
AD7		+	Respiratory failure by aspiration	1,200	3.8	B/IV			T/S
AD8	+		Pneumonia	1,060	8	C/VI	–	+	
PD1		+	Pneumonia	1,330	9.5	B/IV			S/S
PD2	+	+	Pneumonia	1,130	2.5	B/II	–	–	T/S
PD3	+	+	Respiratory failure by aspiration	910	2.5	B/II	–	–	T/S
PD4		+	Colon cancer	1,430	4	A/I			S/S
PD5	+		Pneumonia	1,320	9.3	C/III	–	–	
ALS1	+	+	Respiratory failure	1,480	10.5	0/0	–	–	T/S
ALS2	+	+	Respiratory failure	1,090	1.3	0/I	+	+	T/T
ALS3	+	+	Respiratory failure	1,560	3	0/I	+	+	T/S
ALS4	+	+	Respiratory failure	1,320	10	0/II	+	–	S/S
ALS5		+	Respiratory failure	1,360	2.5	B/I			T/S
ALS6		+	Respiratory failure	1,600	13	B/I			T/S
MSA1	+		Pneumonia, septicemia	1,040	1.5	0/I	–	–	
MSA2	+		Pneumonia	1,090	12	A/I	–	–	

The demographic profile of the cases processed for immunohistochemistry (IHC), quantitative reverse transcriptase-polymerase chain reaction (qPCR), and western blotting (WB) is shown with the case number, the cause of death, brain weight, the postmortem interval, the Braak staging (amyloid deposition/neurofibrillary degeneration), phosphorylated TAR DNA-binding protein-43 (pTDP-43) immunoreactivity in the frontal cortex and the hippocampus, and the p.T185S genotype of the rs3173615 single nucleotide polymorphism. AD, Alzheimer's disease; ALS, amyotrophic lateral sclerosis; MSA, multiple system atrophy; NC, non-neurological causes; PD, Parkinson's disease.

phosphate-buffered saline, the tissue sections were labeled at room temperature for 30 minutes with peroxidase-conjugated secondary antibodies (Nichirei, Tokyo, Japan), followed by incubation with diaminobenzidine tetrahydrochloride substrate (Vector, Burlingame, CA, USA). The sections were processed for a counterstain with hematoxylin. For negative controls, the primary antibody was omitted from the reaction.

Reverse transcriptase-polymerase chain reaction analysis

The source of human neural cell lines processed for reverse transcriptase-polymerase chain reaction (PCR) was described elsewhere. Total cellular RNA was extracted using TRIZOL (Invitrogen, Carlsbad, CA, USA). RNA treated with DNase I was processed for cDNA synthesis using oligo(dT)$_{20}$ primers and SuperScript II reverse transcriptase (Invitrogen). cDNA was then amplified by PCR using HotStar Taq DNA polymerase (Qiagen, Valencia, CA, USA) and a panel of sense and antisense primer sets as follows: 5′-ctgacctgttcatacctgagccat-3′ and 5′-tgggagat atagaccagggttgca-3′ for a 168 base pair (bp) product of the human *TMEM106A* gene (NCBI Reference Sequence Number NM_145041); 5′-aggaagaattcctaggggcaaga-3′ and 5′-atttcacgtcgatagagcgaggga-3′ for a 173 bp product of the human *TMEM106B* gene (NM_018374); 5′-cgtgatttcccac agttccatgag-3′ and 5′-aagtacgtgatcttcagccagtcc-3′ for a

115 bp product of the 3′ noncoding region of the human *TMEM106B* gene (NM_018374); 5′-atacattggcctcatgaccc agag-3′ and 5′-cttgggaacatatgctgtgctctc-3′ for a 140 bp product of the human *TMEM106C* gene (NM_024056); 5′-tgagggacagtactgaagactctg-3′ and 5′-tctgacagggaaggcctt agattg-3′ for a 167 bp product of the human *GRN* gene (NM_002087); 5′-atgaggaggaaggagagaagggga-3′ and 5′-ccttccctttcctgtctgagtctc-3′ for a 188 bp product of the human glial fibrillary acidic protein (*GFAP*) gene (NM_002055); 5′-gagaaaggaacatccggaacagcc-3′ and 5′-tgggagtgccctctcttgctaaca-3′ for a 180 bp product of the human neurofilament, heavy polypeptide (*NFH*) gene (NM_021076); 5′-tacggagcggtcgtgtatcaggat-3′ and 5′-agctgc gtagactctgccgtaact-3′ for a 132 bp product of the human RNA binding protein, fox-1 homolog (*Caenorhabditis elegans*)-3 (*RBFOX3, also named NEUN*) gene (NM_001082575); and 5′-ccatgttcgtcatgggtgtgaacca-3′ and 5′-gccagtagaggcagggatgatgttc-3′ for a 251 bp product of the glyceraldehyde-3-phosphate dehydrogenase (*G3PDH*) gene (NM_002046).

For qPCR, cDNA prepared from frozen human brain tissues and a reference RNA of the human frontal cortex (AM6810; Invitrogen/Ambion) was amplified by PCR in a LightCycler ST300 (Roche Diagnostics, Tokyo, Japan) using SYBR Green I and the primer sets described above. The expression levels of target genes were standardized against the levels of G3PDH detected in the corresponding cDNA samples. All assays were performed in triplicate.

p.T185S genotyping

The rs3173615 SNP composed of p.T185S (C760G) in exon 6 of the human *TMEM106B* gene was studied by direct sequencing of a 226 bp product amplified from brain cDNA by PCR using a primer set of 5′-cagcctatgtcagttatgatg-3′ and 5′-tctgctataacggtaggtact-3′. The representative data are shown in Figure S1a,b,c in Additional file 1.

Vector construction

To study the specificity of anti-TMEM106B antibody, the full-length open reading frame of the human *TMEM106A* gene, the human *TMEM106B* gene, the human *TMEM106C* gene, or the human *GRN* gene was amplified by PCR using PfuTurbo DNA polymerase (Agilent Technologies, Palo Alto, CA, USA) and the set of sense and antisense primers. Subsequently, PCR products were cloned in the expression vector pcDNA4/HisMax-TOPO (Invitrogen) to express a fusion protein with an N-terminal Xpress tag. The vectors were transfected in HeLa cells, SK-N-SH cells, or HEK293 cells using Lipofectamine 2000 reagent (Invitrogen) for transient expression.

Western blot analysis

To prepare total protein extract, cultured cells and frozen brain tissues were homogenized in RIPA buffer (Sigma, St. Louis, MO, USA), NP-40 lysis buffer (homemade), or buffer containing 8 M urea, 2% CHAPS, 0.5% carrier ampholytes pH 4 to 7, 20 mM dithiothreitol supplemented with a cocktail of protease inhibitors (Sigma) – this homogenization was then followed by centrifugation at 12,000 rpm for 10 minutes at room temperature to harvest the supernatant. The protein was separated on 12% SDS-PAGE gel. After gel electrophoresis, the protein was transferred onto nitrocellulose membranes, followed by incubation at room temperature overnight with the anti-TMEM106B antibody A303-439A, rabbit polyclonal anti-TMEM106B antibody raised against a peptide spanning amino acid residues 101 to 200 of the human TMEM106B protein (bs-11694R; Bioss, Boston, MA, USA), rabbit polyclonal anti-TMEM106B antibody raised against the human TMEM106B-GST fusion protein (20995-1-AP; Proteintech, Chicago, IL, USA), or mouse monoclonal anti-Xpress antibody (Invitrogen). The membranes were then incubated at room temperature for 30 minutes with horseradish peroxidase-conjugated anti-rabbit IgG (Santa Cruz Biotechnology, Santa Cruz, CA, USA). The specific reaction was visualized by exposing them to a chemiluminescent substrate (Pierce, Rockford, IL, USA). After the antibodies were stripped by incubating the membranes at 50°C for 30 minutes in stripping buffer, composed of 62.5 mM Tris–HCl, pH 6.7, 2% SDS, and 100 mM 2-mercaptoethanol, the membranes were processed for relabeling with anti-heat shock protein HSP60 antibody (sc-1052; Santa Cruz Biotechnology), serving as an internal control of protein loading. The signal intensity of TMEM106B-immunoreactive bands was quantified using ImageJ software (National Institute of Health, Bethesda, MD, USA), and the expression levels were standardized individually by the corresponding HSP60 signal intensity.

Statistical analysis

The statistical significant difference between two groups was evaluated by Student's *t* test. A significant difference among >2 groups was evaluated by one-way analysis of variance followed by Turkey's *post hoc* test. The differences in the frequency of T185 and S185 isoforms between the groups were evaluated after allocating score 0 to the T185 allele and score 1 to the S185 allele. The correlation between two groups was evaluated by Pearson's correlation coefficient test. $P < 0.05$ in the two-tailed test was considered significant.

Results

Evolutional conservation of TMEM106B

Multiple sequence alignment analysis revealed that the *TMEM106B* gene is highly conserved in various vertebrates through evolution. The amino acid sequence of the human TMEM106B protein was 100%, 96%, 95%, 96%, 95%, 87%, 75%, and 68% identical to the sequences of orthologs derived from *Pan troglodytes*, *Canis lupus familiaris*, *Bos*

Taurus, *Mus musclus*, *Rattus norvegicus*, *Gallus gallus*, *Danio rerio*, and *Xenopus laevis*, respectively (Figure 1a). Furthermore, the amino acid sequence of the human TMEM106B protein was 49% and 47% identical to the sequences of the human TMEM106A and TMEM106C proteins, respectively (Figure 1b), suggesting that the latter two represent paralogues of TMEM106B.

Universal expression of TMEM106A, TMEM106B, TMEM106C, and PGRN mRNAs in human neural cells

By reverse transcriptase-PCR, all cells and tissues examined – including the human cerebrum, astrocytes, neuronal progenitor cells, NTera2 teratocarcinoma-derived neurons, SK-N-SH neuroblastoma, IMR-32 neuroblastoma, U-373MG glioblastoma, T98 glioblastoma, and HMO6 immortalized microglia – expressed varying levels of TMEM106A, TMEM106B, TMEM106C, and PGRN transcripts (Figure 2a,b,c,d, lanes 1,3 to 10). The levels of G3PDH, a housekeeping gene, were almost constant in the cells and tissues examined (Figure 2e, lanes 1,3 to 10). No products were amplified when the reverse transcription step is omitted (Figure 2a,b,c,d,e, lane 2). The expression of TMEM106A, TMEM106B, TMEM106C, and PGRN mRNAs is thus universal in human neural cell lines.

Reduced expression of TMEM106B mRNA in Alzheimer's disease brains

We next analyzed by qPCR the levels of TMEM106B, PGRN, and G3PDH mRNAs in frozen human brain tissues derived from four NC cases, six ALS cases, four PD cases, and seven AD cases presented in Table 1. Before starting this, we investigated the p.T185S genotype of rs3173615 in the human *TMEM106B* gene, on which the T185 isoform acts as a risk factor, while the S185 isoform serves

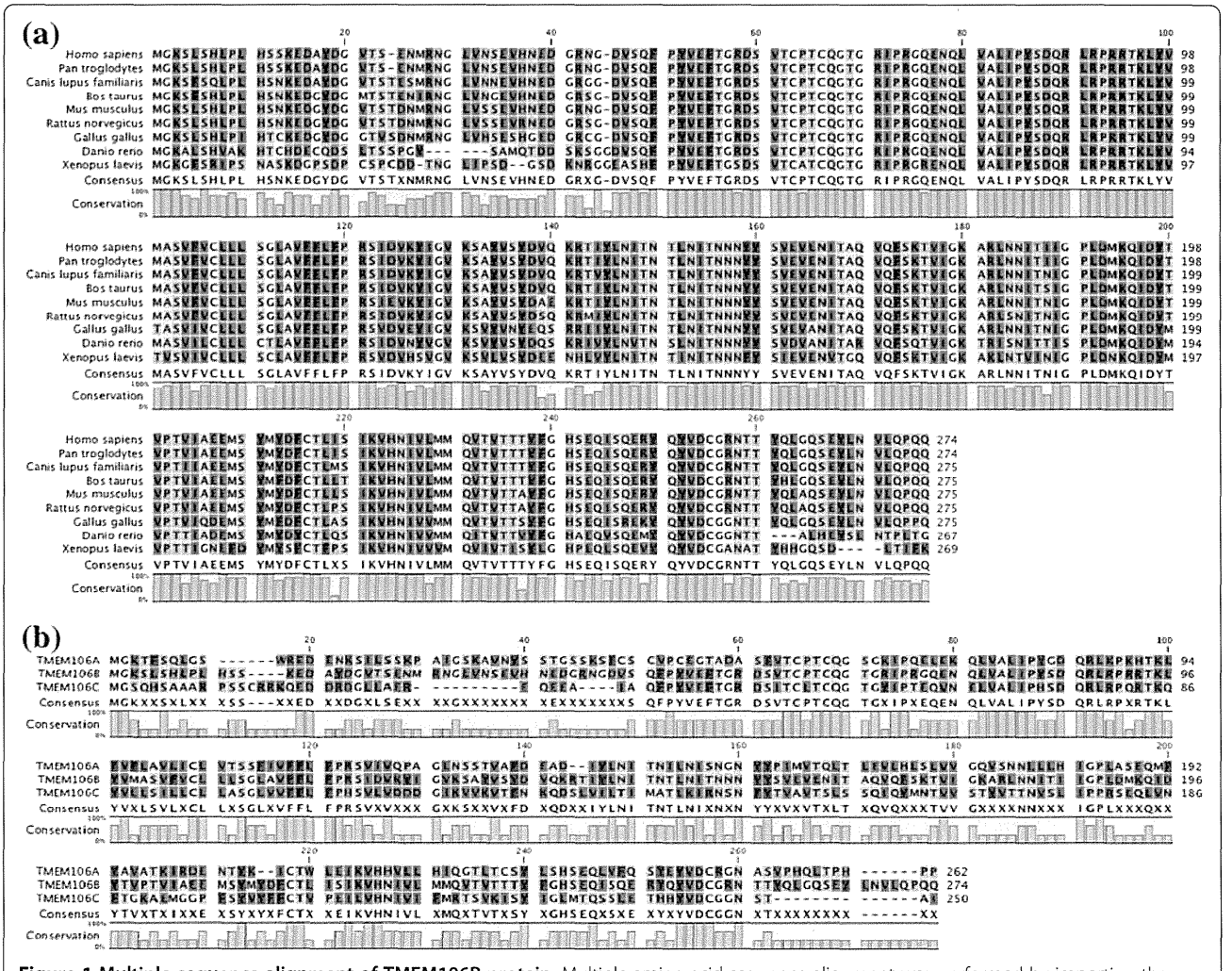

Figure 1 Multiple sequence alignment of TMEM106B protein. Multiple amino acid sequence alignment was performed by importing the corresponding amino acid sequences into CLC Free Workbench (CLC Bio/Qiagen, Aarhus, Denmark). **(a)** Multiple amino acid sequence alignment of TMEM106B orthologs derived from *Homo sapiens*, *Pan troglodytes*, *Canis lupus familiaris*, *Bos Taurus*, *Mus musclus*, *Rattus norvegicus*, *Gallus gallus*, *Danio rerio*, and *Xenopus laevis*. **(b)** Multiple amino acid sequence alignment of the human TMEM106A, TMEM106B, and TMEM106C proteins.

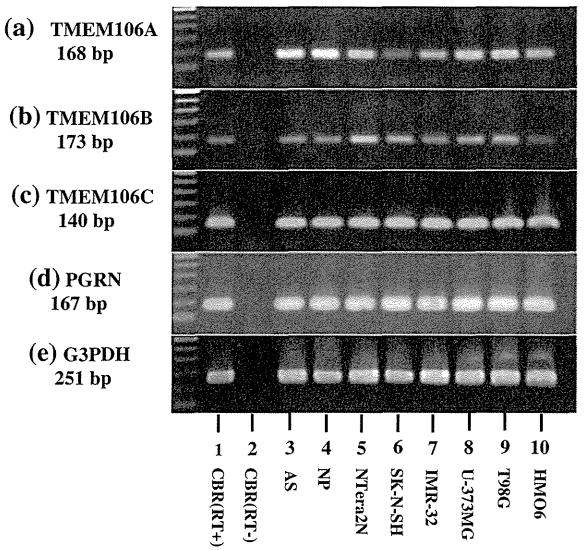

Figure 2 Universal expression of TMEM106B mRNAs in human neural cells. mRNA expression was studied by reverse transcriptase (RT)-polymerase chain reaction (PCR) in human tissues and cultured cells. **(a)** TMEM106A, **(b)** TMEM106B, **(c)** TMEM106C, **(d)** progranulin (PGRN), and **(e)** G3PDH, a housekeeping gene for a positive control. The lanes indicate (1) the frontal cortex of the human cerebrum (CBR) with inclusion of the RT step, (2) CBR without inclusion of the RT step, (3) astrocytes (AS), (4) neuronal progenitor (NP) cells, (5) NTera2 teratocarcinoma-derived neurons, (6) SK-N-SH neuroblastoma, (7) IMR-32 neuroblastoma, (8) U-373MG glioblastoma, (9) T98G glioblastoma, and (10) HMO6 microglia. TMEM106A, TMEM106B, TMEM106C, and PGRN were amplified for 35 cycles, while G3PDH was amplified for 28 cycles.

a protective factor for development of FTLD with *GRN* mutations. In the brains examined, the T185/T185 homozygote consisted of four cases (19.0%), the T185/S185 heterozygote consisted of 14 cases (66.7%), and the S185/S185 homozygote consisted of three cases (14.3%) (Table 1), consistent with the genotyping data of HapMap-JPT [24]. The frequency of T185 and S185 isoforms was thus not significantly different between AD and non-AD groups ($P = 0.6134$).

By qPCR, AD cases showed significantly reduced mRNA levels of TMEM106B, when compared with those in non-AD cases ($P = 0.0035$) (Figure 3a,c). In contrast, AD cases showed significantly elevated mRNA levels of PGRN, with some variations among the cases, when compared with the levels in non-AD cases ($P = 0.0027$) (Figure 3b,d). Notably, a significant negative correlation was found between TMEM106B and PGRN mRNA expression levels (Pearson's correlation coefficient = −0.555; $P = 0.0090$) (Figure 3e). Furthermore, AD cases showed significantly reduced mRNA levels of NFH and elevated mRNA levels of GFAP and NEUN, when compared with the levels in non-AD cases ($P = 0.0003$ for NFH, $P = 0.0004$ for GFAP, and $P = 0.0156$ for NEUN) (Figure 4a,b,c). Importantly, a significant positive correlation was found between TMEM106B and NFH mRNA expression levels (Pearson's correlation coefficient = 0.496; $P = 0.0221$) (Figure 4d).

Moreover, we studied by qPCR the levels of TMEM106A and TMEM106C mRNAs in AD and non-AD brains. Both were markedly elevated in AD brains, compared with the levels in non-AD brains ($P = 0.0002$ for TMEM106A and $P = 0.0005$ for TMEM106C) (Figure S2a,b,c,d in Additional file 2). The expression of TMEM106B paralogues was uniquely regulated in the opposite direction to the expression levels of TMEM106B.

Characterization of the specificity of anti-TMEM106B antibody

The specificity of anti-human TMEM106 antibody was verified by western blot of recombinant human TMEM106A, TMEM106B, and TMEM106C proteins tagged with Xpress expressed in HeLa cells. The A303-439A anti-TMEM106B antibody recognized 45 kDa monomeric and 120 kDa oligomeric forms of TMEM106B tagged with Xpress (Figure 5a, b, lane 3), whereas it did react either with TMEM106A or with TMEM106C (Figure 5a,b, lanes 2 and 4), validating the specificity of the A303-439A antibody. In contrast, both bs-11694R and 20995-1-AP anti-TMEM106B antibodies did not specifically react with the Xpress-tagged human TMEM106B protein (data not shown). We therefore selected A303-439A for western blot and immunohistochemistry analysis in the present study. This antibody specifically reacted with a major 31 kDa protein endogenously expressed in human brain tissues and IMR-32 neuroblastoma cells (Figure 5d, lanes 5 to 7).

Reduced expression of TMEM106B protein in Alzheimer's disease brains

Next, we quantitatively analyzed the levels of TMEM106B, PGRN, and HSP60 proteins in frozen human brain tissues derived from four NC cases, six ALS cases, four PD cases, and seven AD cases, presented in Table 1, by western blot using the A303-439A antibody. AD cases showed significantly reduced levels of TMEM106B, when compared with the levels in non-AD cases ($P = 0.0000004$) (Figure 6Aa,C). AD cases showed a trend for elevated expression levels of PRGN when compared with the levels in non-AD cases, but the difference did not reach statistical significance ($P = 0.5304$) (Figure 6Ba,D). We found no discernible correlation between TMEM106B and PRGN protein expression levels (Pearson's correlation coefficient = −0.242; $P = 0.2912$) (Figure 6E).

Immunohistochemical analysis of TMEM106B expression in Alzheimer's disease and non-Alzheimer's disease brains

We next studied the expression of TMEM106B in the frontal cortex and the hippocampus of six AD cases and 13 non-AD cases, composed of four NC cases, four ALS cases, three PD cases, and two MSA cases, presented in Table 1, by immunohistochemistry using the A303-439A

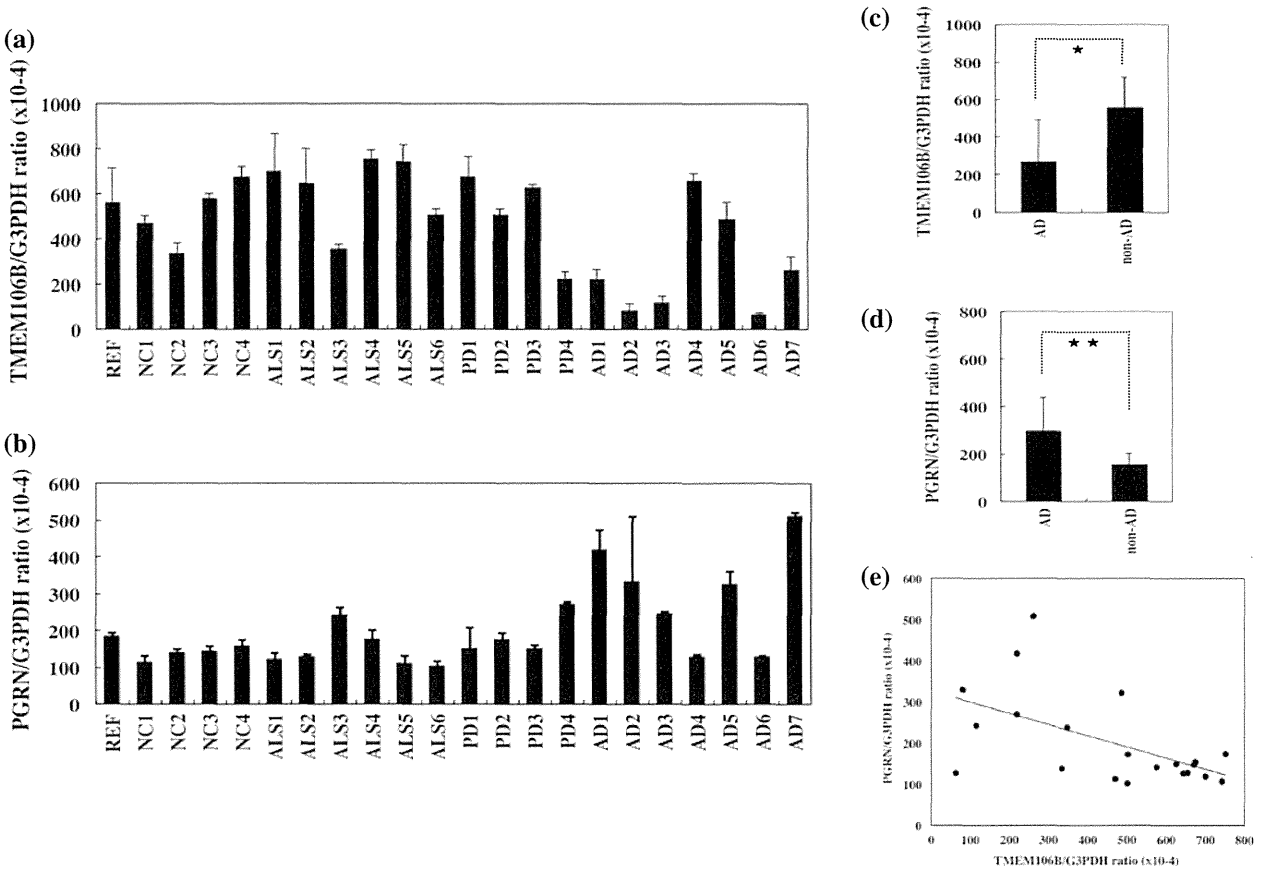

Figure 3 Reduced expression of TMEM106B mRNA in Alzheimer's disease brains. TMEM106B and progranulin (PGRN) mRNA expression levels were studied by quantitative reverse transcriptase-polymerase chain reaction (qPCR) in human brain tissues derived from a reference of the human frontal cortex (REF), four non-neurological control cases (NC), six amyotrophic lateral sclerosis (ALS) cases, four Parkinson's disease (PD) cases, and seven Alzheimer's disease (AD) cases. The expression levels were standardized against those of G3PDH. **(a)** TMEM106B mRNA expression. **(b)** PGRN mRNA expression. **(c)** Difference in TMEM106B levels between AD and non-AD cases. $^{*}P = 0.0035$ by Student's *t* test. **(d)** Difference in PGRN levels between AD and non-AD cases. $^{**}P = 0.0027$ by Student's *t* test. **(e)** Pearson's correlation between TMEM106B and PGRN mRNA levels. Pearson's correlation coefficient indicates −0.555 ($P = 0.0090$).

antibody. Before starting this, we investigated TDP-43 pathology in the brains examined. Among 19 cases, four AD cases and three ALS cases – but no cases of NC, PD, or MSA – showed neuronal or glial pTDP-43 immunoreactivity in the frontal cortex and/or the hippocampus (Table 1; Figure S3a,b,c,d in Additional file 3). In all cases examined, TMEM106B was expressed in the majority of cortical neurons, hippocampal pyramidal neurons and dentate gyrus granule cells, located in the cytoplasm by forming fine granular structures, particularly enriched in the soma and in proximal neurites (Figure 7a,b,c,d). TMEM106B immunoreactivity was occasionally concentrated in the perinuclear region by forming small nodular structures in some populations of hippocampal pyramidal neurons (Figure 7e). Furthermore, subpopulations of oligodendrocytes, reactive astrocytes, and microglia expressed TMEM106B intensely, located in the cytoplasm (Figure 7f; Figure S4b,c in Additional file 4). Neuronal cytoplasmic TMEM106B immunoreactivity was greatly reduced after absorption of the antibody by extract of the Xpress-tagged TMEM106B protein (Figure S4e,f in Additional file 4).

In AD brains, cortical neurons and hippocampal pyramidal neurons were greatly reduced in number, along with substantial reduction of TMEM106B-expressing neurons. However, surviving neurons in AD brains moderately or intensely expressed TMEM106B immunoreactivity in the cytoplasm (Figure 8a,c). Senile plaques were most often unlabeled and rarely faintly labeled by the A303-439A antibody (Figure 8a,e). In contrast, senile plaques, neurofibrillary tangles, and the perivascular neuropil were frequently and intensely labeled with anti-PGRN antibody EPR3781 (Figure 8b,d,f). Some populations of activated microglia also expressed PGRN (Figure S4d in Additional file 4). The vacuoles of granulovacuolar degeneration (GVD)

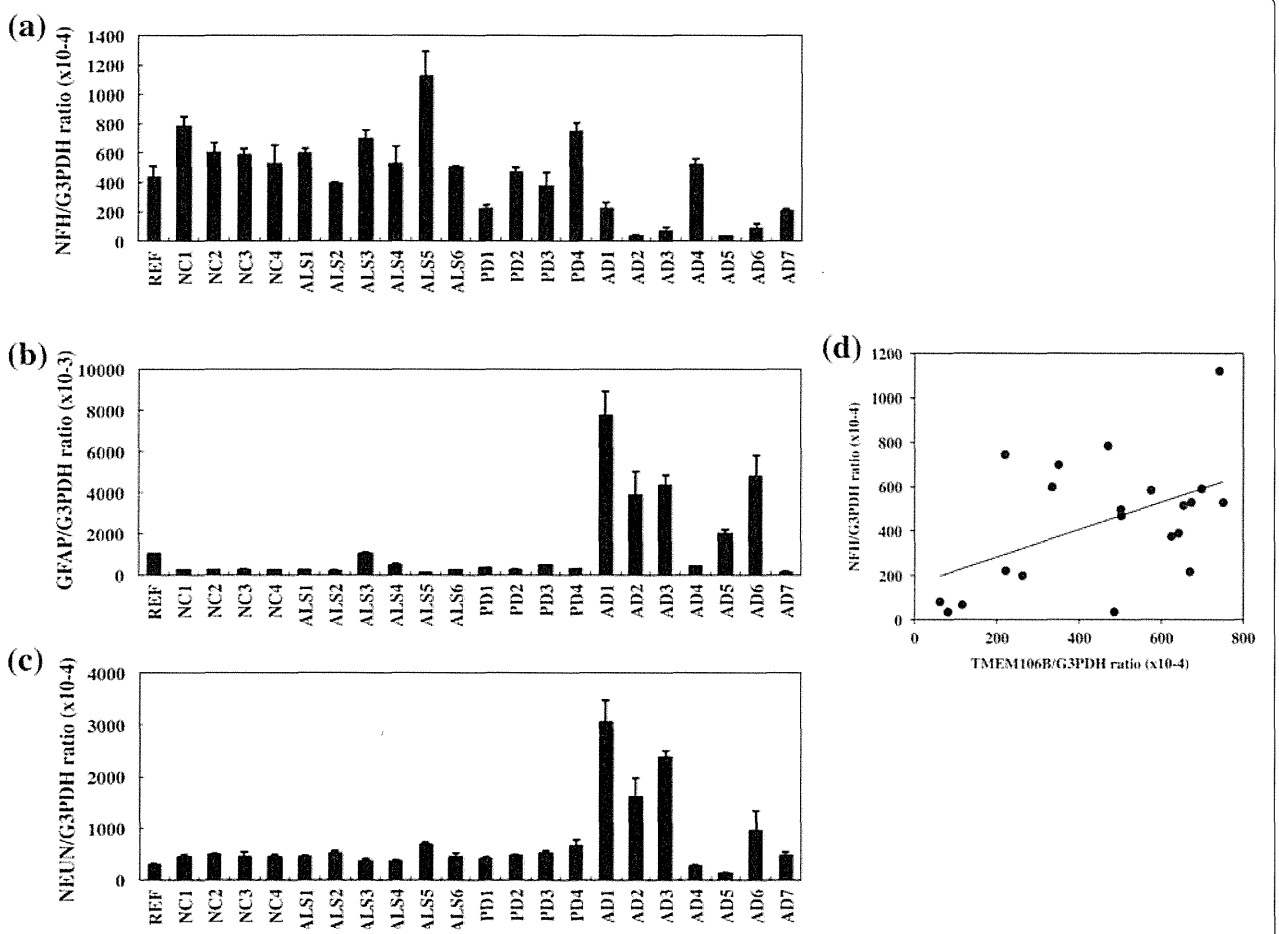

Figure 4 Positive correlation between TMEM106B and neurofilament, heavy polypeptide mRNA levels. Neurofilament, heavy polypeptide (NFH), glial fibrillary acidic protein (GFAP), and RNA-binding protein, fox-1 homolog (*Caenorhabditis elegans*)-3 (RBFOX3, NEUN) mRNA expression levels were studied by quantitative reverse transcriptase-polymerase chain reaction (qPCR) in human brain tissues derived from a reference of the human frontal cortex (REF), four non-neurological causes (NC) cases, six amyotrophic lateral sclerosis (ALS) cases, four Parkinson's disease PD cases, and seven AD cases. The expression levels were standardized against those of G3PDH. **(a)** NFH expression. **(b)** GFAP expression. **(c)** NEUN expression. . **(d)** Pearson's correlation between TMEM106B and NFH mRNA levels. Pearson's correlation coefficient indicates 0.496 ($P = 0.0221$).

often found in pyramidal neurons of the hippocampal CA1 region were devoid of TMEM106B immunoreactivity (Figure S4a in Additional file 4).

Overexpression of TMEM106B and PGRN did not alter their mRNA expression levels

Finally, we studied by qPCR the direct inverse relationship between TMEM106B and PGRN mRNA expression in SK-N-SH neuroblastoma cells following overexpression of Xpress-tagged TMEM106B, PGRN, and LacZ proteins (Figure S5a, lanes 2 to 4 in Additional file 5). Transient overexpression of the TMEM106B, PGRN, or LacZ transgene did not significantly alter the levels of endogenous TMEM106B and PGRN mRNAs ($P = 0.4726$ for TMEM106B and $P = 0.1204$ for PGRN) (Figure S5c,d in Additional file 5). These results suggest that TMEM106B is not directly involved in transcriptional regulation of the *GRN* gene, and *vice versa*.

Discussion

By multiple sequence alignment analysis, we found that the *TMEM106B* gene is highly conserved in various vertebrates through evolution, and it shows substantial homology to both *TMEM106A* and *TMEM106C* genes that represent *TMEM106B* paralogues. Recent studies indicate that TMEM106B plays a pathological role in a wide range of neurodegenerative diseases [17-19,25]. By qPCR, western blot and immunohistochemistry, we studied TMEM106B and PGRN expression levels in a series of AD and non-AD brains. We found that TMEM106B mRNA and protein levels are significantly reduced in AD brains, while PGRN mRNA levels were elevated in AD brains, compared with the levels in non-AD brains. In all brains examined, TMEM106B was expressed in the majority of cortical neurons, hippocampal neurons, and subpopulations of oligodendrocytes, reactive astrocytes, and microglia. These observations largely agree with a recent report

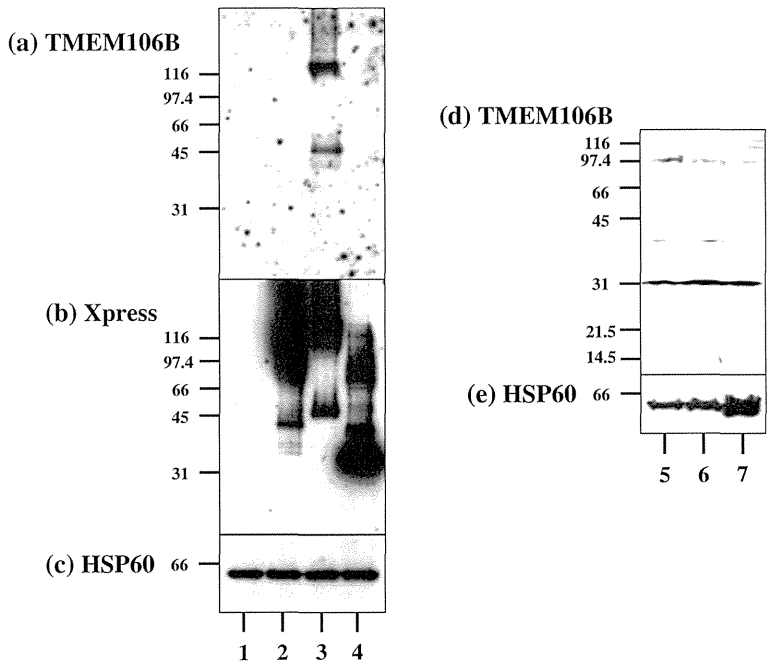

Figure 5 Characterization of anti-TMEM106B antibody. The full-length open reading frame (ORF) cloned in the vector that expresses a fusion protein with an N-terminal Xpress tag was transiently expressed in HeLa cells. Total protein extract was processed for western blot. Lanes represent the protein of (1) untransfected cells and the cells expressing (2) TMEM106A, (3) TMEM106B, or (4) TMEM106C, and the protein of (5) human brain #1, (6) human brain #2, or (7) IMR-32 neuroblastoma cells. Immunoblots of **(a, d)** TMEM106B (the A303-439A antibody), **(b)** Xpress, and **(c, e)** HSP60, an internal control for protein loading.

showing widespread expression of TMEM106B in normal human brains [26]. Although cortical neurons were most evidently lost in AD brains at advanced stages compared with non-AD brains, surviving neurons expressed fairly intense TMEM106B immunoreactivity, suggesting the possibility that reduced expression of TMEM106B in AD brains might simply reflect greater loss of neurons in the cerebral cortex. In contrast, senile plaques, neurofibrillary tangles, and the perivascular neuropil expressed intense PGRN immunoreactivity. These observations are well consistent with previous studies showing enhanced expression of PGRN in microglia, neurons, and neurites surrounding amyloid plaques in AD brains [4,10,27]. Importantly, we found that AD cases show significantly reduced mRNA levels of NFH and elevated mRNA levels of GFAP, when compared with the levels in non-AD cases, reflecting enhanced neuronal loss and astrogliosis in AD brains. Furthermore, we identified a discernible positive correlation between TMEM106B and NFH mRNA expression levels. Unexpectedly, we found a significant elevation in NEUN mRNA levels, a nuclear marker specific for subpopulations of neurons, in AD brains.

The rs1990622 SNP in the *TMEM106B* gene, being in complete linkage disequilibrium with the coding rs3173615 SNP of p.T185S, is closely associated with FTLD-TDP in the patients with *GRN* mutations, who are characterized by lower plasma PGRN levels [3,25]. Previous studies also showed that TMEM106B mRNA and protein levels are elevated in FLTD-TDP brains with *GRN* mutations [1,6]. The expression levels of the risk isoform T185 are much higher than those of the protective isoform S185 owing to destabilization of the S185 protein [3]. Overexpression of TMEM106B inhibits lysosomal function, thereby leading to disturbed turnover of PGRN [8]. An inverse relationship has thus been established in the expression levels between TMEM106B (upregulation) and PGRN (downregulation) in FTLD-TDP. PGRN acts as a pivotal neuronal survival factor, potentially deficient in the brains of neurodegenerative diseases [10,11]. All of these observations suggest that deficient expression of PGRN triggered by elevated expression of TMEM106B promotes neurodegeneration. However, in contrast to FLTD-TDP brains with *GRN* mutations, we found that TMEM106B mRNA and protein levels are reduced in AD brains. In the present study, the frequency of T185 and S185 isoforms was not significantly different between AD and non-AD cases. As a result, we unexpectedly found a reverse inverse correlation between TMEM106B (downregulation) and PGRN (upregulation) in AD brains at least at mRNA expression levels. The possible scenario that TMEM106B plays a protective role against the neurodegenerative processes in AD could therefore be raised, although further studies on *in vitro* and *in vivo* TEME106B knockdown models are required to evaluate this possibility.

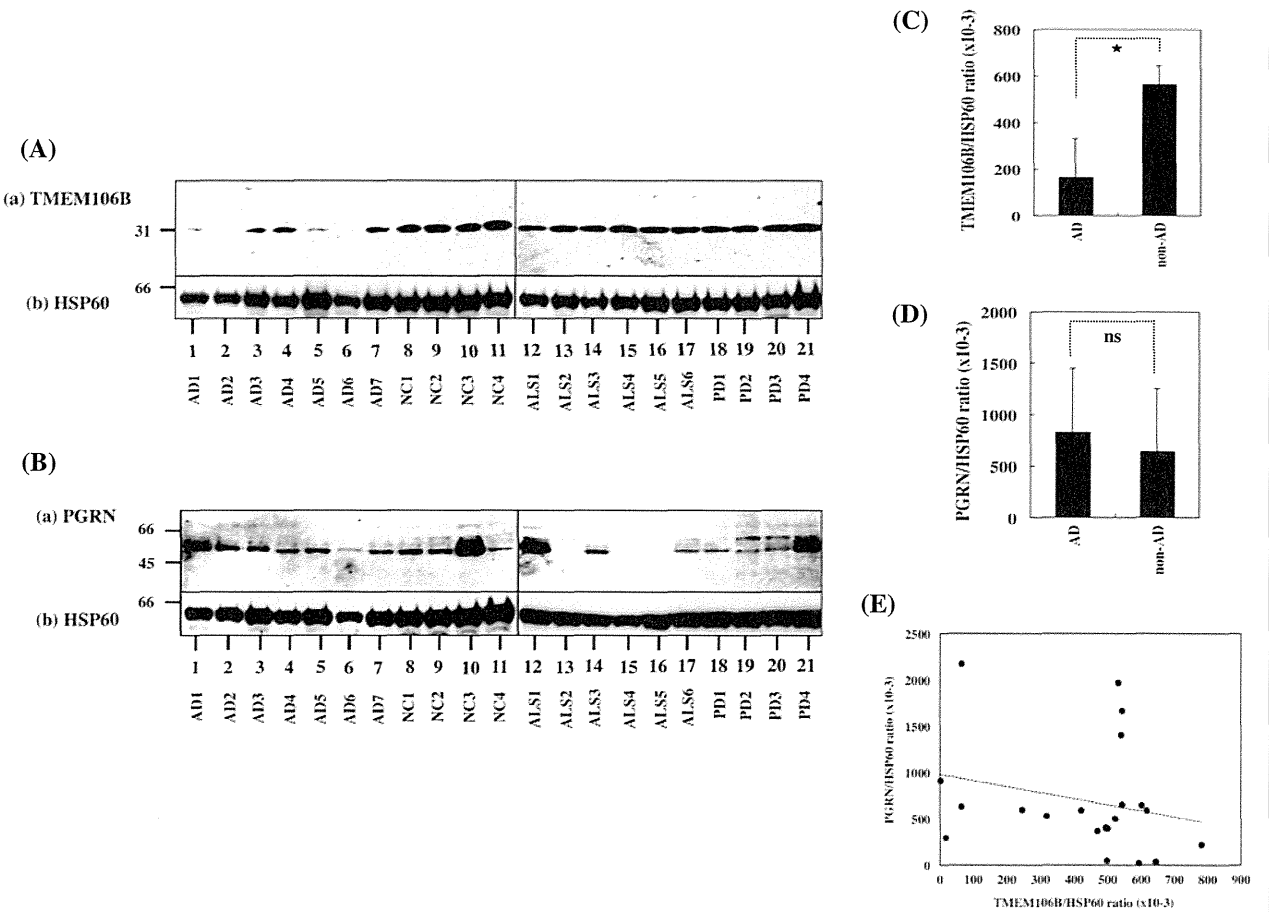

Figure 6 Reduced expression of TMEM106B protein in Alzheimer's disease brains. Protein expression levels were studied by western blot in human brain tissues derived from four non-neurological causes (NC) cases, six amyotrophic lateral sclerosis (ALS) cases, four Parkinson's disease (PD) cases, and seven Alzheimer's disease (AD) cases. The expression levels were standardized against those of HSP60. **(A)** TMEM106B expression: **(a)** TMEM106B and **(b)** HSP60. **(B)** Progranulin (PGRN) expression: **(a)** PGRN and **(b)** HSP60. **(C)** Difference in TMEM106B levels between AD and non-AD cases. *$P = 0.0000004$ by Student's *t* test. **(D)** Difference in PGRN levels between AD and non-AD cases. ns, non-significant ($P = 0.5304$ by Student's *t* test). **(E)** Pearson's correlation between TMEM106B and PGRN protein levels. Pearson's correlation coefficient indicates −0.242 ($P = 0.2912$).

In the present study, AD cases showed significantly elevated mRNA levels of PGRN, when compared with the levels in non-AD cases. However, we did not find a significant elevation of PGRN protein levels in AD brains, leading to no obvious inverse correlation between TMEM106B and PGRN protein expression levels. The inconsistency between PGRN mRNA and protein levels is attributable to the complex post-transcriptional modification of the PGRN protein. The PGRN protein contains 7.5 tandem repeats of 12 cysteinyl motifs separated by linkers. When secreted extracellularly, PGRN – cleaved by elastase and matrix metalloproteases within linker regions – generates several smaller fragments called granulins (GRNs), composed of GRN A to G and paragranulin or epithelins.

Importantly, the full-length PRGN and its cleaved fragment GRNs play a discrete role in regulation of various biological responses [10,11]. PGRN exhibits neurotrophic and anti-inflammatory activities, whereas GRNs serve as a proinflammatory mediator. Expression levels of PGRN, whose release is facilitated by anti-inflammatory stimuli in microglia, are elevated in multiple sclerosis brains [28,29]. Astrocytes produce large amounts of secretory leukocyte protease inhibitor, a negative regulator of proteolytic processing of PGRN, in response to proinflammatory stimuli [28]. In contrast, PGRN acts as a chemotactic factor for microglia capable of producing large amounts of reactive oxygen species, although microglia, following exposure to PGRN, show an enhanced capacity to phagocytose amyloid-$\beta_{1\text{-}42}$ [30]. At present, therefore, whether upregulated expression of PGRN in AD brains plays a neuroprotective or neurotoxic role remains unknown. We found that overexpression of either TMEM106B or PGRN transgene in SK-N-SH neuroblastoma cells does not immediately affect endogenous levels of PGRN or TMEM106B mRNA, excluding the direct interaction

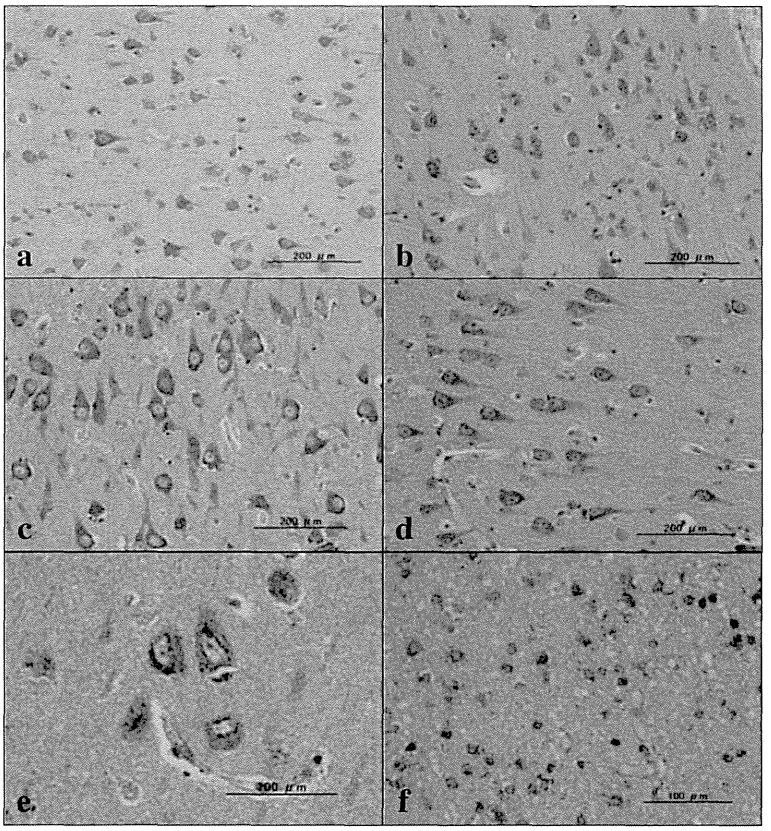

Figure 7 TMEM106B immunoreactivity in non-Alzheimer's disease brains. Expression of TMEM106 immunoreactivity was studied in 13 non-Alzheimer's disease brains presented in Table 1 by immunohistochemistry using the A303-439A antibody. **(a)** Non-neurological causes (NC), the frontal cortex, cytoplasmic staining of cortical neurons; **(b)** amyotrophic lateral sclerosis (ALS), the frontal cortex, cytoplasmic staining of cortical neurons; **(c)** NC, the hippocampal CA1 region, cytoplasmic staining of pyramidal neurons; **(d)** ALS, the hippocampal CA1 region, cytoplasmic staining of pyramidal neurons; **(e)** NC, the hippocampal CA1 region, intense staining of small nodular structures accumulated in the perinuclear region of pyramidal neurons; **(f)** NC, the frontal white matter, cytoplasmic staining of oligodendrocytes, reactive astrocytes, and microglia.

between both in transcription regulation of mutual genes. It is worthy of note that TMEM106B is co-localized with PGRN within the endosome/lysosome compartments [3], and treatment with inhibitors of lysosomal acidification, such as bafilomycin A1, ammonium chloride, and chloroquine, elevates TMEM106B levels in mouse neural cells [8].

A recent study found that the frequency of the protective C allele on rs1990622 in the *TMEM106B* gene, showing the complete linkage disequilibrium with p.T185S on rs3173615 [3,13,15], is reduced in AD cases exhibiting TDP-43 pathology [18]. In contrast, we found no difference in the frequency of T185 and S185 isoforms on rs3173615 between AD and non-AD cases. TDP-43, a nuclear RNA/DNA-binding protein capable of interacting with UG/TG repeat stretches of target RNAs/DNAs, plays a key role in regulation of transcription, alternative splicing, mRNA stability and transport, and microRNA biogenesis, actively involved in the pathogenesis of FTLD/ALS termed TDP-43 proteinopathy [31]. Because TMEM106B is identified as a direct target for TDP-43-regulated gene expression [32], the cytoplasmic sequestration of TDP-43 in TDP-43 proteinopathy might induce deregulated expression of TMEM106B in neurons containing TDP-43-positive inclusions. In the present study, four out of six AD cases showed TDP-43 pathology in the frontal cortex and/or the hippocampus. Among these we found that three cases (AD1, AD3, and AD6) show markedly reduced TMEM106B mRNA and protein expression levels (see Figures 3a, 6A), suggesting an involvement of aberrant regulation of the *TMEM106B* gene by TDP-43 in the pathogenesis of AD, although larger cohorts are required to evaluate this possibility.

In contrast to downregulation of TMEM106B expression, the expression of two paralogues of TMEM106B (TMEM106A and TMEM106C) was markedly upregulated at mRNA levels, almost specifically expressed in AD brains. The corresponding genes are located in different chromosomes – that is, TMEM106A (17q21.31), TMEM106B (7p21.3), and TMEM106C (12q13.1) – whose expression is presumably regulated by distinct mechanisms. The possibility exists that upregulation of the functionally relevant paralogues reflects a compensation for a deficiency of